A Physiological Mathematical Model of the Pulmonary Respiratory System

A Physiological Mathematical Model of the Pulmonary Respiratory System

PhD Thesis by

Mads Lause Mogensen

Center for Model-Based Medical Decision Support
Department of Health Science and Technology
Aalborg University, Denmark

River Publishers
Aalborg

ISBN 978-87-92329-97-4 (e-book)

Published, sold and distributed by:
River Publishers
P.O. Box 1657
Algade 42
9000 Aalborg
Denmark

Tel.: +45369953197
www.riverpublishers.com

Table of Contents

Abstract

In patients where mechanical ventilation is required, the aim of mechanical ventilation is to ensure adequate gas-exchange while avoiding ventilator induced lung injury (*VILI*). Uncertainties exist regarding the causes and prevention of *VILI*. The effect of mechanical ventilation on the distribution of ventilation, perfusion and gas-exchange in the lungs is not fully understood; especially the effect of gravity is debated in the literature. Furthermore, it has not been determined how alveoli behave during mechanical ventilation and it has not been determined to which extend alveoli opens and close during breathing even for healthy lungs. The first step towards improving ventilator therapy strategies is therefore to understand how the healthy lungs respond to mechanical ventilation. The focus of this PhD project was to develop a mathematical physiological model of the respiratory system consisting of four sub models describing the pulmonary ventilation, perfusion, blood chemistry and gas-exchange during mechanical ventilation. The ventilation model simulates pressure-volume relationships in the lungs and the perfusion model describes the pulmonary perfusion during mechanical ventilation both models being stratified with respect to the effects of gravity. The blood model describes acid-base chemistry of the blood. The gas-exchange model simulates oxygen and carbon dioxide distributions in the respiratory system and simulates e.g. arterial oxygen and carbon dioxide levels during tidal breathing. The models are validated against experimentally obtained data and simulate well a wide range of physiological parameters during breathing. The model has indicated that alveoli in the healthy subjects do not collapse. Furthermore, simulation results show that gravity affects the gas exchange more than what is experimentally observed. This leaves room to speculate that other effects such as anatomical gradients, hypoxic vasoconstriction and bronchodilation may compensate for the effects of gravity on the regional ventilation and perfusion of the lungs.

Danish Summary/ Dansk Resumé

En af de primære livsreddende terapiformer på en intensivafdeling er mekanisk ventilation. Terapien og indstillingen af respiratoren er imidlertid kompliceret af modstridende kliniske mål. På den ene side skal patienterne være tilstrækkeligt oxygeneret, men samtidig kan overdreven brug af positiv end expiratory pressure (*PEEP*), tidal volumen og inspireret iltfraktion medfører ventilator induced lung injury (*VILI*). Terapi med mekanisk ventilation er endvidere kompliceret af en manglende forståelse af hvordan respiratoren påvirker ventilationen, perfusion and gas-udvekslingen lokalt i lungerne. Der er endnu ikke opnået enighed i litteraturen om hvorvidt de mindste lungeenheder (alveolerne) kollapser under normal vejrtrækning samt hvilken effekt tyngdekraften har på det respiratoriske system. Det første skridt mod en bedre behandling af mekanisk ventilerede patienter er at opnå en fuldendt forståelse af de raske lunger. Denne PhD-afhandling, som er basseret på seks artikler, omhandler udviklingen og brugen af matematiske fysiologiske modeller til at undersøge effekten af mekanisk ventilation på raske personer. Den udviklede model består af fire grundmodeller af henholdsvis den pulmonære ventilation, perfusion, gas-udveksling samt blodets syre/base kemi. Den lagdelte ventilationsmodel beskriver de lokale tryk-volumen forhold i lungerne og indeholder en beskrivelse af luftvejsmodstanden, brystvæggens elasticitet, lungevævets visko-elastiske egenskaber, effekten af surfaktant, samt de hydrostatiske effekter i lungerne. Perfusionsmodellen beskriver den lokale perfusion i lungerne under mekanisk ventilation og inkluderer en beskrivelse af den arteriolemodstand, kapillærerelasticitet og modstand, blodviskositet samt længde og antal af lungekapillærer. Ydermere er der lavet antagelser om trykprofilen i den pulmonale arterie. Modellen af blodets syre/base egenskaber beskriver transporten af ilt og kuldioxid i blodet og inkluderer en beskrivelse af Bohr-Haldane effekten. Modellen af gas-udvekslingen inkluderer de andre tre grundmodeller og beskriver ilt og kuldioxid distributionen i det respiratoriske system, hvilket vil sige transporten mellem omgivelserne, det anatomiske dead space, alveolerne, kapillærerne, samt det arterielle og venøse blod. Den samlede model er valideret mod en række eksperimentelle data fundet i litteraturen. Modelsimuleringerne er i god overensstemmelse med en bred vifte af disse

fysiologisk målte parametre under normal vejrtrækning. F.eks. er modellen i overensstemmelse med globale tryk-volumen kurver, distribution af lungedensitet, ventilation og perfusion, total kapillærerperfusion, transition time af de røde blodlegemer, arterielle og venøse partialtryk af ilt og kuldioxid. Resultaterne præsenteret i denne afhandling indikerer, at alveolerne hos raske personer ikke kollapser under normal vejrtrækning. Endvidere har modelsimuleringerne vist at den oprejste lunge ikke er i stand til at opretholde tilstrækkelig gasudveklsing og ilting af det arterielle blod. Det er derfor indikeret at effekten af tyngdekraften bliver modvirket af andre mekanismer f.eks. hypoktisk vasokonstriktion og bronkodilation.

Preface

This thesis presents my work done during my PhD-study started in October 2009 and finished February 2011. The work was done at the Center for Model-based Medical Decision Support, Department of Health Science and Technology, Aalborg University, Denmark. The title of the thesis is A Physiological Mathematical Model of the Respiratory System. The thesis has four chapters: introduction, model development and implementation, summary of papers, and discussion and conclusion. The introduction offers a general introduction to the main motivation and the subject of the thesis i.e. understanding of ventilation, perfusion and gas-exchange of the human lungs during mechanical ventilation. It gives a brief overview of the literature on the subject and outlines the methodological approach applied in the studies presented in this thesis. Furthermore the chapter introduces the concepts and state of the art within the field of mathematical modelling of the respiratory system. The model development and implementation describes the overall solution strategy and model structure. The summary of papers presents six papers that constitute the basis of this thesis. The discussion and conclusion section provides a discussion of the main findings of the work and its relation to previous work, suggests future work, and briefly concludes all work presented in the thesis.

Remember that all models are wrong; the practical question is how wrong do they have to be to not be useful.

George Edward Pelham Box
Empirical Model-Building and Response Surfaces (74), 1987

Acknowledgements

This PhD-thesis is the result of 2 years of intensive work started during my Master's Program [1, 2]. A number of people have provided their knowledge and support, and they have each played an important role in this work. First, I would like to thank my friends and family, for their support and understanding whenever I was excited or discouraged due to work breakthroughs or difficulties. Staff at Center for Model-based Medical Decision Support, academic as well as administrative deserves thanks for being good colleagues and for welcoming me going from being a masters' student to being a PhD-student. In this regard, I would like to express my special appreciation of Steen Andreassen and Dan Stieper Karbing for their support and comments regarding research, writing, and life in general. Also, Line Rugholm Sanden should receive my thanks for keeping me company in the office. I would also like to thank Lars Pilegaard Thomsen for excellent help in the laboratory. My co-author Kristoffer Lindegaard Steimle, should receive a special thanks for his invaluable help in making the studies possible as well as for his comments to the manuscripts.

SUPERVISORS

- **Steen Andreassen**, Dr. Tech., PhD, Center for Model-based Medical Decision Support, Department of Health Science and Technology, Aalborg University.
- **Dan Stieper Karbing**, PhD, Center for Model-based Medical Decision Support, Department of Health Science and Technology, Aalborg University.

Mads Lause Mogensen
Aalborg, February 2011

List of Papers

This paper is based on six listed papers, which will be referred to in the text by their corresponding roman numericals:

Paper I: Andreassen, S., Steimle, K.L., Mogensen, M.L, de la Serna, J.B., Rees, S.E. and Karbing, D.S. (2010), The Effect of Tissue Elastic Properties and Surfactant on Alveolar Stability, *J. Appl. Physiol.* 109(5): 1369-1377.

Paper II: Steimle, K.L., Mogensen, M.L., Karbing, D.S. and Andreassen, S. (2010) A Model of Ventilation of the Healthy Human Lung. *Comput. Methods. Programs. Biomed.* 101(2): 144-155.

Paper III: Mogensen, M.L., Thomsen, L.P., Karbing, D.S. Steimle, K.L., Zhao, Y., Rees, S. E., Andreassen, S. (2010). A Mathematical Physiological Model of the Dynamics of Pulmonary Ventilation. *UKACC International Conference on Control, CONTROL 2010, 7-10 September 2010, Coventry, UK*: 734-739.

Paper IV: Mogensen, M.L., Steimle, K.L., Karbing, D.S., and Andreassen, S. (2010). A Model of Perfusion of the Healthy Human Lung. *Comput. Methods. Programs. Biomed.* 101(2): 156-165.

Paper V: Mogensen, M.L., Karbing, D.S. and Andreassen, S. (2011). The Effect of Arteriolar Resistance on Perfusion Distribution in a Model of the Pulmonary Perfusion. *18th World Congress of the International Federation of Automatic Control (IFAC) August 28 - September 2, 2011, Milano, Italy.* (Submitted)

Paper VI: Mogensen, M.L., Karbing, D.S., Steimle, K.L., Rees, S.E. and Andreassen, S. (2011). The Effect of Gravity on Pulmonary Gas Exchange – A Modelling Study. (Submitted)

Chapter 1.

Introduction

In this chapter the problems related to mechanical ventilation in the intensive care unit are presented. The chapter includes a description of the concepts of pulmonary ventilation/perfusion ratio, which is one of the major factors determining gas-exchange in critically ill patients. Pulmonary ventilation and perfusion are influenced by the mechanics of the lungs. A description of the most important mechanical properties of the respiratory system determining the ventilation (surfactant, tissue elasticity, chest wall elasticity, airway resistance, visco elastic properties of the lungs) and perfusion (pulmonary arterial pressure, viscosity of the blood, arteriolar resistance and capillary elasticity) are therefore introduced. This is followed by a description of factors that affect distribution of ventilation and perfusion (gravity, pulmonary vasoconstriction, anatomical and geometric gradients) in the lungs. The chapter also includes a description of the concept of physiological mathematical modelling, which is a key concept in this study.

1.1 MECHANICAL VENTILATION

Mechanical ventilation has saved countless lives for about 50 years and today, mechanical ventilation is the second most frequent therapeutic intervention after treatment of cardiac arrhythmias in the intensive care unit (*ICU*) [3]. In case of severe lung injuries such as patients with acute respiratory distress syndrome (*ARDS*) or acute lung injury (*ALI*), finding the appropriate settings on the ventilator is of great importance [4]. Evidence from randomized, controlled clinical trials, e.g. [5-8], has shown that specific ventilator management strategies can reduce mortality, length of *ICU* stay, and cost. Figure 1.1 shows the dilemma faced by clinicians when finding appropriate ventilator settings. At one side sufficient gas-exchange must be obtained by mechanical ventilation to secure the patients are properly oxygenated and CO_2 eliminations is optimized. Usually this is done by an increase in the minute volume, $\dot{V}_{Total}$, by either increase the tidal volume, V_T, or the

breathing frequency, f, ($\dot{V}_{Total} = f \cdot V_T$) adding a positive end expiratory pressure, *PEEP*, increasing inspired oxygen fraction, F_iO_2, or turning the patient to prone position [9, 10]. However, as with any other therapy, mechanical ventilation may unfortunately expose patients to side effects. So at the other hand, excessive use of pressures, tidal volumes and high F_iO_2 may cause alveolar rupture, inflammation and oxygen toxicity also named ventilator induced lung injury, *VILI*.

In addition to the mentioned ventilator settings (V_T, f, *PEEP* and F_iO_2) conventional ventilators have several other settings and modes (e.g. ratio between inspiration and expiration time, *I:E*), that also affects gas-exchange of the patients. However, of the available settings, *PEEP* and tidal volume may be considered as the most complex to optimize. *PEEP* improves gas-exchange by preventing alveolar collapse, recruiting alveoli, redistributing fluid in the alveoli and avoiding shunt, but excessive *PEEP* can increase pressure to harmful levels where *VILI* occurs. In addition high *PEEP* levels might reduce the alveolar capillary perfusion by compression of pulmonary capillaries within interalveolar septa. The setting of tidal volume is currently based on a lung protective strategy with low volumes of about 6 to 8 ml/kg [4]. Despite of guidelines based on lung protective strategy, the management strategy of ventilator support still remains under debate e.g. [4, 8, 11-13] and how to achieve the primary goal of improving oxygenation while ensuring that the lungs heal properly is still not fully understood [14-16].

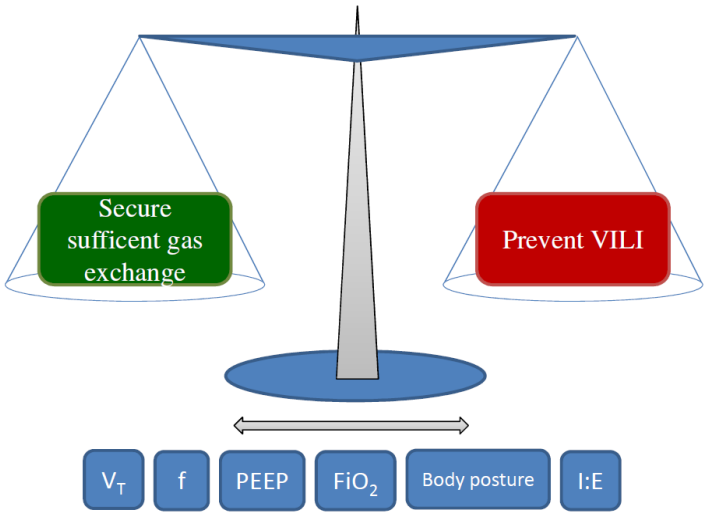

Figure 1.1 The tradeoff between ensuring sufficient gas-exchange while avoiding ventilator induced lung injury (*VILI*) when mechanically ventilating critically ill patients. Boxes illustrate that doctors have to optimize different ventilator settings and body posture considering the balance between achieving sufficient gas-exchange and preventing *VILI*. V_T: Tidal volume. f: Breathing frequency. *PEEP*: Positive end-expiratory pressure. F_iO_2: Inspired oxygen fraction. *I:E*: Ratio between inspiration and expiration time.

One of the reasons that finding appropriate ventilator settings may be so difficult is illustrated in Figure 1.2. Pulmonary gas-exchange is determined by the interaction between alveolar ventilation and pulmonary perfusion and is further complicated by the chemical properties of blood, which causes the exchange of O_2 and CO_2 to interact through the Bohr-Haldane effect [17-20]. Currently there is no complete understanding of how ventilation and perfusion are affected by different ventilator settings and since these effects often counteract, it is very difficult to predict the effect of various types of mechanical ventilations on gas-exchange.

The prediction of the effects of mechanical ventilation is further complicated by the fact that matching between pulmonary ventilation and perfusion, also known as the $\dot{V}/Q$ -ratio unfortunately is not the same throughout the lungs. Thus, as illustrated in Figure 1.3, some alveoli might be more perfused than ventilated and some might be more ventilated than perfused, whereas others might be equally perfused and ventilated and have a $\dot{V}/Q$ -ratio close to 1. Figure 1.3 is a simulation results of a model that will be discussed in details later in this thesis [21-25].

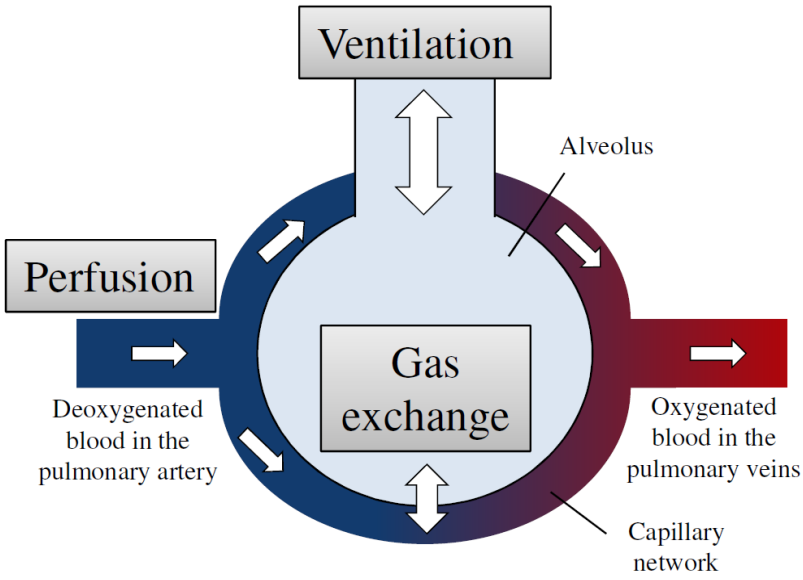

Figure 1.2 Gas-exchange in alveoli is a complex interaction between ventilation of air and perfusion of blood to the alveoli.

As shown in Figure 1.3 matching between ventilation and perfusion determines partial pressures of O_2 and CO_2 in the alveoli and since discrepancy between $\dot{V}/Q$ increases with disease it is one of the major factors determining gas-exchange in critical patients at the *ICU* [26].

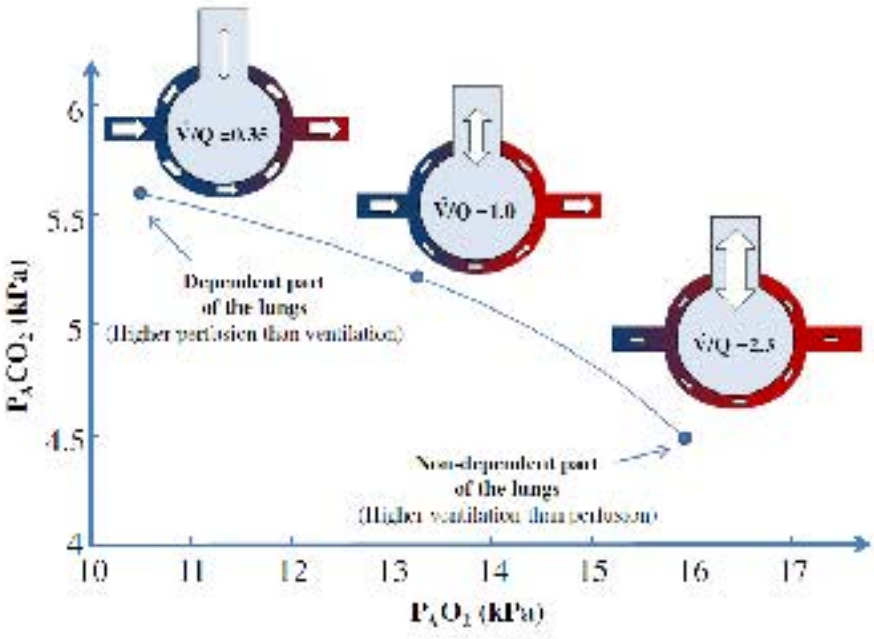

Figure 1.3 Simulated relationship between alveolar partial pressure of O_2 and CO_2 for a healthy subject in upright position. Indicated is also the ventilation/perfusion ratio.

The mechanical properties of the respiratory system determine how alveoli behave during breathing. It is therefore these properties that determine perfusion and ventilation of the individual alveoli. The following sections will illustrate the fundamental mechanical properties of the respiratory system that determines local alveolar ventilation, perfusion and gas-exchange.

1.2 LUNG MECHANICS

Mechanical changes in lung structure during respiration also known as lung mechanics have been widely discussed in the literature e.g. [27-34]. However, no established unifying theory currently exists. Much of the uncertainty has been due to the difficulties in documenting alveolar and capillary mechanics, given the small size and large movement during breathing. This section introduces the most important mechanical components of the respiratory system starting with those determining alveolar ventilation. This is followed by an introduction to mechanics determining pulmonary perfusion.

1.2.1 Static Lung Mechanics Determining Alveolar Ventilation

Lung mechanics affecting alveolar ventilation are often described by pressure-volume (*PV*) relationships as the ones illustrated in Figure 1.4. Figure 1.4-A shows a simulated *PV*-curve of a pair of excised lungs ventilated with either saline or air. The simulations are performed with the model that will be discussed later in this thesis [21-23]. The simulated *PV*-curves are similar to those found in the literature e.g. [28, 35-37]. By comparing static *PV*-curves from excised saline-filled and air-filled lungs, two fundamental components of the respiratory system can be identified, namely the effect of tissue elasticity and the effect of surface tension determined by surfactant. Surfactant molecules act on the air/water interface inside the alveolar epithelium and reduce the surface tension and hereby the work of breathing. Furthermore surfactant maintains fluid balance across the alveolar membrane and prevents alveolar collapse. In saline filled lungs the air-liquid interface is abolished and the effect of surfactant is therefore eliminated. Since surfactant is one of the main contributors to the hysteresis observed on the *PV*-curve, saline filled lungs have no hysteresis when inflated and deflated.

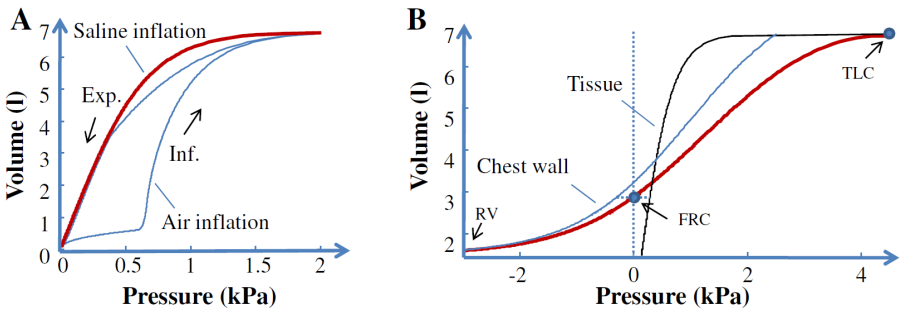

Figure 1.4 Simulated pressure-volume relationship of an isolated lung inflated with saline (Thick line) or air. B: Simulated total pressure-volume curve (Thick line) including the effect of chest wall and lung tissue elasticity. RV: Residual volume. FRC: Functional residual capacity. TLC: Total lung capacity.

The effect of chest wall (abdomen and rib cage) is eliminated when isolated lungs are ventilated as the lungs simulated in Figure 1.4-A. Figure 1.4-B shows a simulated *PV*-curve from lungs inside the chest wall filled with saline. The figure shows that the total static *PV*-curve of the respiratory system without surfactant (Thick curve) is a sum of the pressure generated by the chest wall and the pressure generated by lung tissue. The sigmoid shape of the total *PV*-curve therefore reflects the balance of forces within the lungs. At functional residual capacity (*FRC*) the negative pressure generated by the chest wall is counterbalanced by the positive pressure from the lung tissue.

Global *PV*-curves can be obtained from both healthy and ill subjects [27, 38-42]. They are global in the way that they are obtained at the mouth and therefore is the sum of local conditions within the lungs. As is the case with $\dot{V}/Q$ -ratio, alveolar pressures are not the same throughout the lungs due to gravitational forces [43-45]. In spite of this, global *PV*-curves can be considered as consisting of three segments separated by two inflection points [27, 46-48]. Figure 1.5 shows a simulated global *PV*-curve of a healthy subject ventilated from residual volume, *RV*, to total lung capacity, *TLC*. The simulation was performed with the same model as used for the simulations shown in Figure 1.3 and Figure 1.4. The simulated global *PV*-curve is similar to those obtained experimentally e.g. [22, 49]. On the inflation curve a segment with low compliance can be identified. The segment is separated from an intermediate segment with greater compliance by a lower inflection point (*LIP*). This steeper part of the curve is followed by an upper inflection point (*UIP*) beyond which the curve flattens again. As indicated on Figure 1.5 it can be hard to find the exact position of the inflexion points and many of the techniques described in the literature rely on eye detection, which is subject to interobserver variability. Interpretation of the same *PV*-data by different clinicians has been observed to differ as much as 1.1 kPa [50].

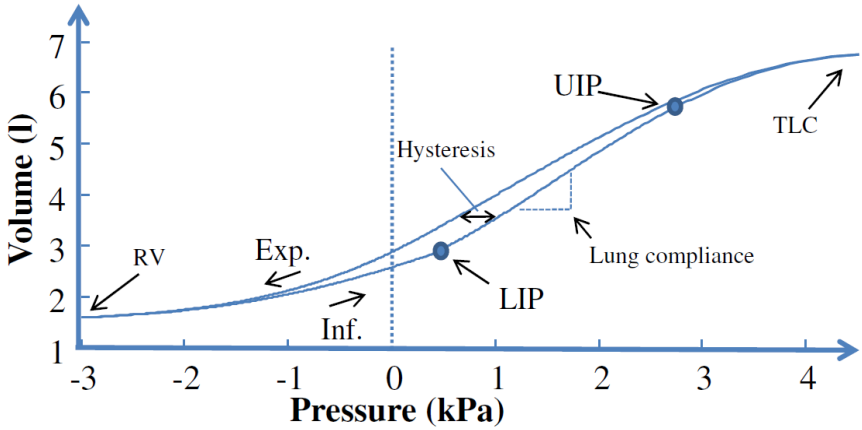

Figure 1.5 A simulated total pressure-volume curve from residual volume (RV) to total lung capacity (TLC) of a healthy subject. Indicated is the lung hysteresis, lung compliance, upper inflection point (UIP) and lower inflection point (LIP).

A number of studies have tried to explain the meaning of the global *PV*-curve and the inflexion points the interpretation of the *PV*-curve, however, remains under debate e.g. [4, 38, 51-53]. Some authors (e.g. [27, 38]) have regardless of the problems with global measurements interpreted the first segment with low

compliance to represents filling of derecruited or collapsed alveoli. The second segment with high compliance is suggested to represent a continuous recruitment of alveoli and isotropic expansion of the already open alveoli. The last segment is claimed to represent a gradual cessation of recruitment where harmful pressure levels and *VILI* occurs. The concept of the global *PV*-curve representing recruitment (opening) and derecruitment (closing) of alveoli must, however, be interpreted with some caution. In addition to the global measurements, there are still conflicting data on how alveoli behave during breathing. Schiller et al. [54] showed three behaviors of alveoli during mechanical ventilation, those that do not change in size, those that change size throughout the entire inflation, and those that pop open at a certain pressure and rapidly change size. These observations support the theory of recruiting and derecruiting alveoli. On the other hand Hubmayr [55] criticized this theory and concluded that *PV*-curve from *ARDS* patients can be obtained without having alveoli open and close, but rather forcing air into open, but liquid filled alveoli.

1.2.2 Dynamic Lung Mechanics Determining Alveolar Ventilation

Along with the static components, dynamic airway resistance and viscoelastic properties of the lungs are also known lung mechanics that affect the ventilation [56-59]. Figure 1.6 shows a typical gas flow and airway pressure profile during constant flow inflation from a subject being mechanical ventilated [60]. The figure illustrates the airway resistance and viscoelastic properties of the respiratory system. After end inspiration there is a sudden initial pressure drop from P_{Max} to P_1, which is due to the dissipation of airway resistance. The initial pressure drop is followed by a slower, secondary pressure drop to a static plateau, which is believed to be caused by either stress adaptation of the lung tissue including surfactant or pendelluft due to ventilation inhomogeneity [61]. The effects of viscoelasticity and pendelluft are hard to distinguish, however, in the normal healthy lungs pendelluft has been proven to have a minimal contribution to stress relaxation [57]. Zhao et al. [42] recently presented a simple, rapid (20 seconds) method for measuring both the viscoelastic and resistive properties of the respiratory system from a single long inflation-deflation maneuver. The results confirm previous observations [31, 49, 62-64] that stress adaption due to viscoelasticity increase non-linearly with inflation volume and airway pressure.

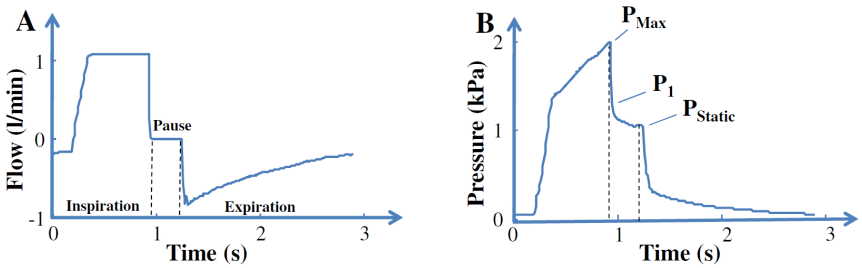

Figure 1.6 Measured flow of gas (A) and pressure measured at the mouth (B) during a constant flow inflation, with a period of zero flow (pause) followed by a passive expiration [22]. During the pause period the airway pressure rapidly drops from its maximum value, PMax, to P1, this is followed by a slower decrease to an apparent static plateau, PStatic.

1.2.3 Mechanics Determining Pulmonary Perfusion

The pulmonary capillaries wrap each alveolus in a fine and dense mesh that covers about 70 % of the alveolar wall [65]. The network forms a continuous sheet of blood around the alveoli, which maximizes gas-exchange. The pulmonary perfusion through the capillaries and the rest of the pulmonary vessels is among others determined by circuit resistance and pressure differences between the arterial and venous end of the system. Pressure at the venous side is almost constant and changes only with the depth of the lungs due to the hydrostatic gradient, which increases down the lungs due to gravity. The important pressure is therefore the pressure at the arterial end. Arterial pressure is not constant, according to the pressure exerted by the heart; it rises during ventricular systole and falls during ventricular diastole. Due to low peripheral resistance, the pulsating transmission of pressure from the right ventricle to the arterioles and capillaries leads to a highly pulsating perfusion in the capillaries [66]. Mean pressure in the pulmonary circulation drops from about 2.2 kPa in the pulmonary artery to 1.2 kPa in the pulmonary vein. The arterioles and capillaries accounts for an equal pressure drop of approximately 0.5 kPa [61]. From Poiseuille's law stated in *Eq.* 1 it can be identified that pulmonary resistance, R, is determined by viscosity of the blood, η_{Blood}, lengths, L, and radii, r, of the pulmonary vessels, assuming that pulmonary perfusion can be approximated by a fully developed laminar flow in a straight uniform tube.

$$R = \frac{8 \cdot L \cdot \eta_{Blood}}{\pi \cdot r^4} \qquad (1)$$

The erythrocytes that transport most of the oxygen in the blood typically compose 45 % of the blood volume and greatly influence the viscosity of blood [67]. Erythrocytes are highly deformable biconcave disks measuring approximately 2 by

8 µm in unstressed state. They can squeeze through round capillaries down to a diameter less than 3 µm [68]. In the 1930's Fahraeus and Lindqvist [69] measured blood viscosity of human blood in cylindrical glass tubes with different sizes and found that viscosity of blood changes with diameter of the tube. The change of viscosity can be explained by the arrangement of the erythrocytes. As illustrated in Figure 1.7 erythrocytes in capillaries below 10 µm are arranged in a single-profile flow with a sleeve of plasma in the zone between erythrocytes and wall where the sheer force is maximal. A decrease in vessel diameter below 5 µm increases the viscosity dramatically, because the tubes become too narrow for the erythrocytes to squeeze through. Flow in tubes with greater diameters becomes more multi-profile and the erythrocytes will travel in different streamlines with different velocities. As a consequence of this irregular movement the internal friction between erythrocytes and vessel wall increases, leading to a viscosity increase as the diameter increases. [68, 70, 71]

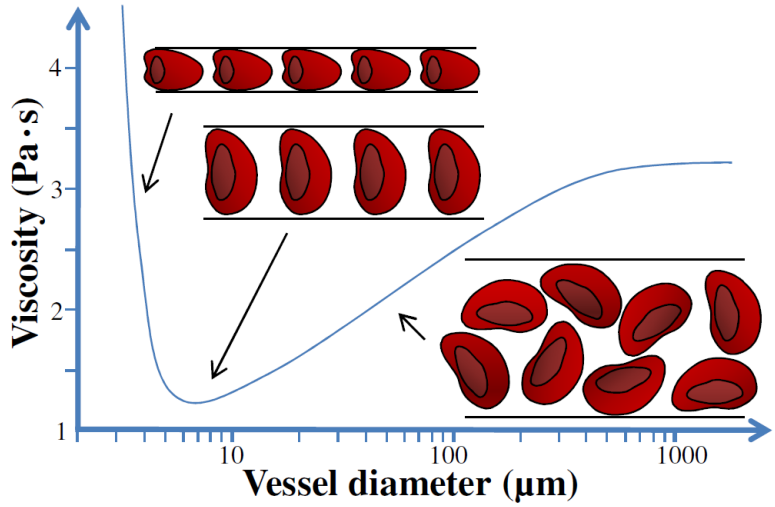

Figure 1.7 Viscosity as a function of vessel diameter for blood with a hematocrit of 45% simulated with a model by Pries et al. [71]. Illustrations of the blood flowing from left to right through tubes with different diameters.

In addition to the mechanical properties directly linked to the blood, also radius, length and number of the blood vessels are also essential for the pulmonary resistance. Especially the radius that is raised to the power of four in (1) is important. A change in transmural pressure over the vessel wall, P_{TM}, will change the radius according to the vessel elasticity. The elasticity of the especially the capillaries is therefore an important factor of the pulmonary circulation [72].

In summary lung mechanics affecting ventilation is a composition of several components that all affect the *PV*-relationship in the lungs. The most important components determining pulmonary ventilation are: lung tissue elasticity, surface tension determined by the effects of surfactant, chest wall, gravity and anatomy of the lungs, dynamic airway resistance and viscoelastic properties of the lungs. The most important factors determining the pulmonary perfusion are: pressures differences between arterial and venous side, pressure exerted by the heart, pulmonary resistance determined by viscosity, length, number and elasticity of the blood vessels.

Due to the complexity of the interaction of these components of the respiratory system that is further complicated by changes at different disease stages we do still not know how alveoli behave during mechanical ventilation even in the healthy lungs and how this affects the gas-exchange between air in the alveoli and blood in the capillaries.

1.3 DISTRIBUTION OF VENTILATION AND PERFUSION IN THE LUNGS

As described above it is currently hard to predict how different ventilator settings affect the respiratory system. A regional insight into lung mechanics and the distribution of ventilation and perfusion could therefore improve the current understanding and potential be helpful in the future management of respiratory failure therapy in the *ICU*. This section introduces the current knowledge, uncertainties and illustrates some of the key factors that may influence distribution of ventilation and perfusion in the lungs.

As a consequence of the lungs being the largest and only organ in the body containing air filled alveoli it has large intravascular hydrostatic and extra-alveolar pressure gradients down the lungs. During breathing the lungs are expanding and compressing under its own weight, changing both densities and pressure gradients from top (non-dependent part) to bottom (dependent part). The effect of gravity in human lungs was first studied by West and his colleagues in the 1960's [44, 45, 73]. They showed with radioactive gases that both ventilation and perfusion were greater in the dependent part of the lungs. This increase in ventilation and perfusion from top to bottom of the lungs has also been demonstrated in more recent studies using other techniques e.g. positron emission tomography, PET [74-76]. Figure 1.8 shows simulated ventilation, perfusion and $\dot{V}/Q$ -distribution down the lungs performed with the model that will be described in details later. $\dot{V}/Q$ -ratio decreases from the top towards the bottom. Despite inhomogeneities of a factor of about 3-4 between the non-dependent and dependent $\dot{V}/Q$ -ratio [74-77], ventilation and perfusion are generally agreed to be well matched in normal subjects [65, 78, 79].

Due to the work by West and his colleagues in the 1960's, gravity has long been thought of as the main determinant of the distribution of ventilation and

perfusion in the lungs. Improved imaging methods (e.g. single photon emission computed tomography**,** *SPECT* [80, 81], *PET* [82], high resolution computed tomography, *HRCT* [83], microspheres [84, 85]) with high spatial resolution have, however, demonstrated that regional distribution of ventilation and perfusion are quite heterogeneous at the same vertical height (*isoheight*). Some authors (e.g. Glenny et al. [84]) have therefore stated that gravity is a minor determinant of the distribution of perfusion and ventilation. This controversial statement is supported by the fact that the vertical gradient does not apply irrespective of posture [77, 81] and that a vertical gradient is present at zero gravity [86]. Different speculative mechanisms determining the vertical distribution have been suggested. A passive anatomical gradient due to geometries of the pulmonary vascular and airway trees has been postulated [84, 87]. Active mechanisms are also claimed to redistribute air and blood within the lungs. For instance vasoconstriction [88-90] and bronchodilation [91] are observed in hypoxic and hypercapnic areas of the lungs. Hypoxic pulmonary vasoconstriction and hypercapnic pulmonary vasoconstriction are contractions of the smooth muscles in the wall of the small arterioles. The contraction actively redistributes blood from hypoxic and hypercapnic areas to better ventilated areas of the lungs. The exact mechanism of the response is not known in spite of numerous studies e.g. [88-90]. However, it is agreed upon that nitric oxide synthesis [92] plays an important role in this active redistribution of both blood and air in experiments with abnormal hypoxic and hypercapnic levels. However, it has not been determined to which extent active redistribution of blood and air is present in the healthy and sick lungs.

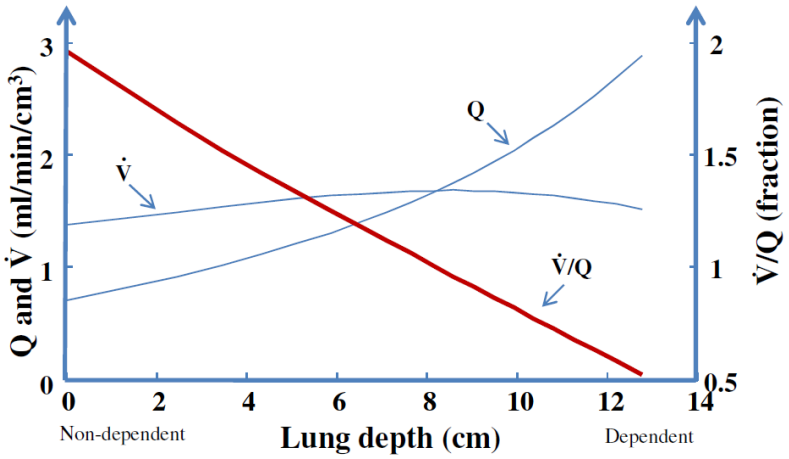

Figure 1.8 Model simulated distribution of ventilation ($\dot{V}$) and perfusion (Q) and $\dot{V}/Q$-ratio from non-dependent to dependent part of the lungs similar to the one observed by West and his colleagues in the 1960's [44, 45].

In conclusion it has not been determined to which extent passive or active mechanisms interact with gravity and how they influence the regional distribution of ventilation and perfusion. The discussion whether gravity or something else determines the distribution of ventilation and perfusion is therefore still going on e.g. [43, 93-95]. Since passive (including gravity) and active mechanisms are hard to separate in experimental setups their individual interactions are even more speculative than their existence. As will be described below, mathematical models are a way to explore and explain the connections between these complex properties of the lungs.

1.4 PHYSIOLOGICAL MATHEMATICAL MODELLING

Mathematical modeling of physiological systems is a craft of interdisciplinary fields that applies fundamental laws of mathematics, physics, chemistry, and engineering to characterize the interactions of physiological subsystems. Such models are useful tools in various applications in medicine including respiratory physiology [96]. As shown in Figure 1.9 a mathematical physiological model is developed as a set of equations and model parameters which take a number of inputs e.g. pressure exerted by the ventilator and inspired oxygen level. These model equations then generate outputs such as alveolar ventilation, $\dot{V}_A$, arterial blood pressure of oxygen, P_aO_2, $\dot{V}/Q$ -relationship and so on.

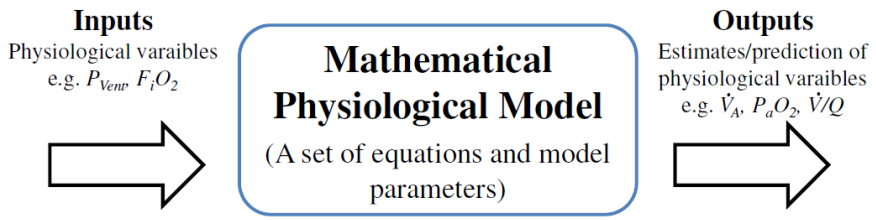

Figure 1.9 A schematic diagram of the inputs and outputs to a mathematical and physiological model.

Modelling has three advantages in science according to Kansal et al. [97]. First a model can be based on many experimental studies, providing a joint interpretation of these data. Second, the process of bringing together data from different studies into one model can reveal gaps in our knowledge of the system. Third, a model that fits reality can help researchers in testing new hypotheses.

Carson et al. [98, 99] divide the general purpose of development of models into three categories: descriptive, explanatory and predictive models. Descriptive models are a way of mathematically describing a system or relationship shortly and

accurately, for instance a linear equation describing a proportional relationship between two parameters. Explanatory models can explain some connections among different parameters and structures in a system. This can improve the understanding of the system, or this type of model can be used as a hypothesis that can be tested against experimental data. Explanatory models can also be used for estimating parameters that cannot otherwise be measured using only the available variables as input. The predictive model can determine how a system would react to a change or stimulus, for instance how the human lungs would respond to a change in respirator treatment.

1.5 STATE OF THE ART IN MODELS OF THE RESPIRATORY SYSTEM

The respiratory system has been modelled and studied in the past from different perspectives and at different levels of detail. Within gas-exchange, some of the simplest models use the concepts of continuous ventilation and perfusion describing gas mixing and pulmonary gas-exchange, see e.g. [12, 96, 100]. These models are sometimes referred to as gill models, since they model the concept of fish gills, with a continuous flow of water over the filaments and a continuous flow of blood through the laminae mounted on them [101]. Whilst these models describe the physiological processes in an intuitive way, they do, however, neglect that human ventilation and perfusion is not continuous but tidal in nature [65, 102, 103]. Other models including non-physiological analogies like springs and dashpots for the lungs exists e.g. [56, 96, 104], however, they do not improve our understanding of the local behavior of the respiratory system either. Other more detailed models have focused either exclusively on airway and lung mechanics [105-108], gas-exchange [102, 109, 110] or pulmonary circulation [87, 111, 112] without coupling them. Liu et al. [113] was the first to combine airway mechanics, gas-exchange and perfusion in a nonlinear model of the normal human lungs. However the model still describes the lungs as a lumped single compartment unable to describe local behavior of e.g. ventilation and perfusion in the lungs.

The Nottingham Physiology Simulator is another physiological model that combines: cardiovascular, acid-base, respiratory, cerebrovascular and renal physiology [114-117]. The Nottingham Physiology Simulator is a stratified model from the non-dependent to the dependent part of the lungs capable of reproducing typical clinical data (e.g. partial pressures of O_2 and CO_2 in the arterial and mixed venous blood). However, in order to investigate whether gravity alone can describe the distribution of ventilation and perfusion the model must be expanded with several important physiological aspects such as the effect of surfactant, pulsatile blood flow, changes in lung density during tidal breathing and the Bohr-Haldane effect.

To summarize, several models have been developed to describe different aspects of the respiratory system, but none couples airway and lung mechanics, gas-exchange and pulmonary circulation in a way that clarifies the effects of

gravity on the local ventilation, perfusion and gas-exchange for different ventilator settings.

1.6 AIM OF STUDY

In the previous sections it was reviewed that patients in the *ICU* with severe lung injuries have reduced lung function and therefore often require mechanical ventilation. Appropriate ventilator settings are of crucial importance to reduce the risk of *VILI*, and to minimize the duration of mechanical ventilation and improve mortality. Currently, the management of the ventilator settings is difficult and based on limited understanding. The effects of different ventilator settings on the respiratory system are not fully understood and more knowledge is needed concerning mechanical properties of the lungs that affect local distribution of ventilation, perfusion and gas-exchange, especially the effects of gravity. Furthermore we currently do still not know how alveoli behave during mechanical ventilation and it has not been determined to which extend alveoli opens and close during breathing even for healthy lungs.

Mathematical models can be used to explore and clarify complex properties of the lungs. This implies a need for a novel mathematical model describing the entire respiratory system enabling simulation of the effects of mechanical ventilation on distribution of ventilation, perfusion and gas-exchange. Such a model would potentially close the gap in our understanding of local ventilation and perfusion. In the future this could assist doctors and other medical personnel in reducing ventilator associated lung injury and might prove to be a powerful tool for choosing appropriate ventilator settings.

The first step in this direction is to fully understand how the healthy human lungs behave. Hence this study aims at developing a mathematical physiological model describing the distribution of ventilation, perfusion and gas-exchange in the lungs of a healthy human subject. In order to describe ventilation in the lungs properly, the model should include the most important lung mechanics components of the respiratory system i.e. lung tissue elasticity, surface tension determined by the effects surfactant, chest wall elasticity, gravity, airway resistance and viscoelastic properties of the lungs. In order to describe pulmonary perfusion the model should include a description of: pressure exerted by the heart, pulmonary resistance determined by viscosity, length and elasticity of the blood vessels.

By including the effect of gravity as the only determinant for the distribution of ventilation and perfusion, the model can clarify to which extend gravity may affect the distribution of ventilation and perfusion and if other passive or active mechanisms should be included to redistribute air and blood in the lungs. The model therefore firstly omits speculative mechanisms as geometries of the pulmonary vascular and airway trees, hypoxic vasoconstriction and bronchodilation.

On this basis, the PhD-thesis aims to answer the following three research questions:

1. *Can a physiological mathematical model be developed which describes the distribution of ventilation, perfusion and gas-exchange in the healthy human lungs?*
2. *How do alveoli behave during breathing in healthy lungs – do they collapse?*
3. *Can gravity alone describe the ventilation and perfusion distribution down the lungs – or should additional active or passive component be included in the model?*

In the terminology of Carson et al. [98, 99], the primary goal for the desired model of the respiratory system is to be an explanatory model. Explaining how alveoli behave and how gravity affects the respiratory system. As a secondary goal the model should also be predictive in the sense that changes in ventilation, perfusion and gas-exchange could be predicted in response to changes in ventilator settings.

Chapter 2.

Model Development and Implementation

This chapter describes the overall model structure and the connection between the model components, before going into details with them individually.

2.1 MODEL COMPONENTS

In order to answer the three main research questions a physiological mathematical model of the healthy lungs is constructed. Figure 2.1 shows the main components included in the model. The model simulates a paralyzed subject during mechanical ventilation, pressure generated by the respiratory muscles is therefore firstly neglected. Pressure exerted by the ventilator is given as input to the model. During inspiration the ventilator exerts a positive pressure that forces air through the anatomical dead space, *AD*, into the alveoli, *A*. During expiration the positive ventilator pressure is removed and the lungs exhale according to the mechanics of the lungs. The model includes a description of the airway resistance. The lungs are divided into a number of horizontal layers, N_{Layer}, distributed from the non-dependent part (i=1) to the dependent part (i= N_{Layer}) of the lungs. In this way each layer reflects a lung depth corresponding to a hydrostatic pressure. The hydrostatic pressure is caused by the lung tissue weighting down on the layers below due to gravity. Blood in the capillary network also imposes a hydrostatic gradient that increases the blood pressure down the lungs. In addition to the ribs that illustrates chest wall elasticity also surfactant lining inside the alveoli, lung tissue elasticity and viscoelastic properties are included in the model.

The transfer of respiratory gasses between alveoli air and capillary blood (gas-exchange) is a passive process of diffusion that is mainly determined by capillary transition time of the erythrocytes and the diffusing capacity [61, 118]. In this model equilibrium is assumed, such that end-capillary blood has the same partial pressures of O_2 and CO_2 as the alveoli air. Pulsatile pulmonary capillary perfusion at different lung depths, Q_i, is simulated during tidal breathing. The model includes

a physiological description of the capillary elasticity and resistance, viscosity of the blood, number and length of lung capillaries and pulmonary arterial pressure, P_{pa}, driven by the heart. The model, furthermore, includes a uniform pulmonary arteriolar resistance throughout the lungs. A constant fraction of the total cardiac output, Q_{Shunt}, is not involved in gas exchange and mix with the pulmonary end-capillary blood on the arterial side of the circulation. It is assumed that the simulated resting healthy subject has a constant elimination of CO_2 and consumption of O_2 ($\dot{V}_{CO2}$, and $\dot{V}_{O2}$). A model of acid/base chemistry of the blood including the Bohr-Haldane is used for calculation of the partial pressures of O_2 and CO_2 in the capillary, arterial and venous blood [17, 19].

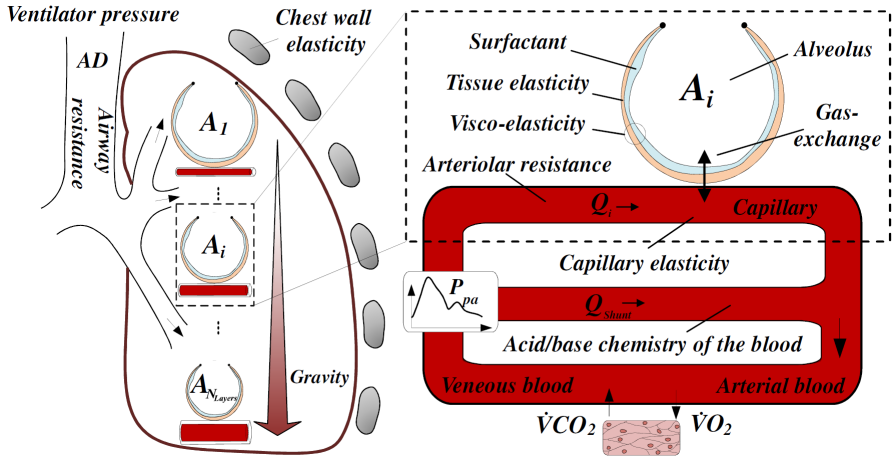

Figure 2.1 Illustration of model components included in the total lung model. The lungs are divided into a number of horizontal layers, N_{Layers}. Shown are the anatomical dead space, AD, alveoli at layer i, A_i, capillaries, arterial and venous blood. Physiological components included are the ventilator pressure, airway resistance, gravity, chest wall elasticity, surfactant, tissue elasticity, viscoelastic properties of the lungs, gas-exchange, arteriolar resistance, capillary elasticity, pulmonary arterial pressure, P_{pa}, perfusion at layer i, Q_i, shunt, Q_{Shunt}, acid/base chemistry of the blood, tissue elimination of CO_2 and consumption of O_2, $\dot{V}_{CO2}$, and $\dot{V}_{O2}$.

The total model of the respiratory system is divided into four sub models described in details in six papers: 1) A model of pulmonary ventilation; 2) a model of pulmonary perfusion; 3) a model of blood acid/base chemistry; 4) a model of gas-exchange. Figure 2.2 shows the four sub models. The important physiological components included in each of the sub models are listed in the model boxes. The solid arrows between the boxes indicate that the gas-exchange model incorporates the models of ventilation, perfusion and blood acid/base-chemistry. The dashed

arrow between the ventilation model and the perfusion model indicates that the models interact with each other through the extra alveolar pressure, which is the pressure outside the alveoli and capillaries. The extra-alveolar pressure is the sum of the hydrostatic pressure and the pressure exerted by chest wall. In the boxes it is also indicated in which papers the individual model parts are described. The individual physiological components are introduced below in order to give the reader an overview of the model components, before each paper is presented in a summary.

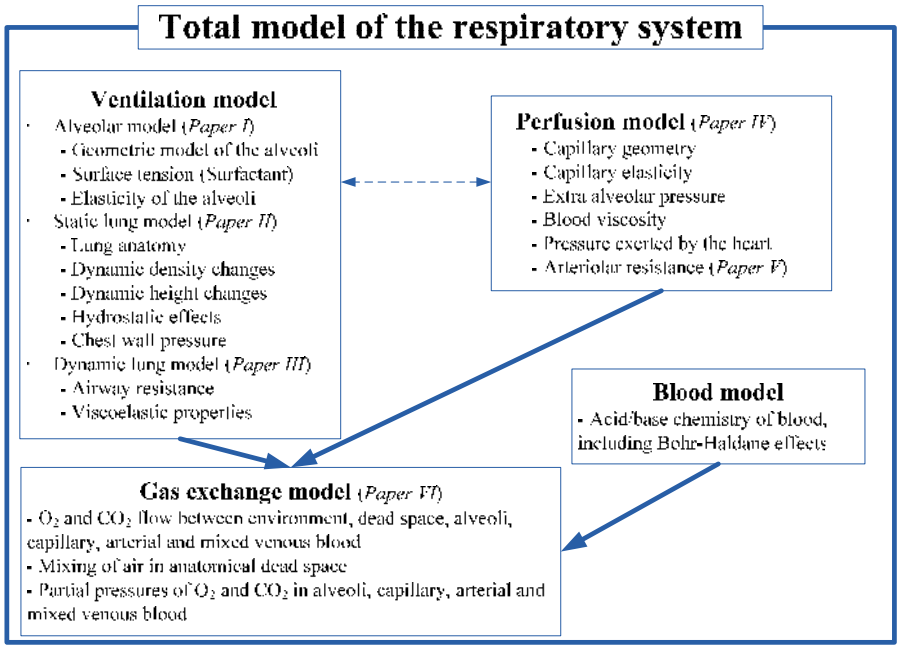

Figure 2.2 The lung model is composed of four sub models i.e. a model of pulmonary ventilation, a model of pulmonary perfusion, a model of blood acid/base-chemistry and a model of gas-exchange. The sub models each include a number of physiological components that are listed in the model boxes. In the figure it is also indicated in which paper the different parts of the models are described. The dashed arrow shows the link between the ventilation model and the perfusion model through the extra alveolar pressure and the effect of capillary blood on lung density. The full arrows indicate that the gas-exchange model incorporates the other three sub models.

2.1.1 Ventilation Model

The ventilation model includes a description of the physiological model components that affect alveolar ventilation during tidal breathing. The total

ventilation model is described in *Papers I* to *III*, which can be seen as a chronological development of the model. *Paper I* introduces lung mechanics that affect ventilation at the level of an alveolus i.e. the effects of surfactant and alveolar shape upon the surface pressure and the static elastic properties of the alveolar wall. *Paper II* expands this model by incorporating the model of an alveolus into a model of the entire lung. This includes a description of lung anatomy, effect of chest wall elasticity and hydrostatic gradient caused by the weight of lung tissue and blood. *Paper II* also describes changes in the hydrostatic pressure gradients due to variations in lung density and height during breathing. *Paper III* finalizes the ventilation model by describing the dynamic lung mechanics regarding airway resistances and viscoelastic properties of the lungs. The paper also describes how the dynamic model parameters are identified and how the model is validated against experimentally measured flow, volume and pressure profiles obtained from five healthy subjects at rest.

2.1.2 Perfusion Model

The perfusion model describes physiological components affecting pulmonary perfusion, this work is described in *Paper IV* and *Paper V*. Geometry and elastic properties of the pulmonary capillaries are described in details in *Paper IV*. This paper also includes a description of how the blood flows, including the effects of blood viscosity, capillary elasticity and the pressure at the proximal end of the capillary. The model of the capillary perfusion also describes the lungs as divided into layers distributed from the non-dependent part to the dependent part of the lungs. In this way the distribution of perfusion down the lungs can be simulated. As *Paper IV* will show, the capillary model overestimates the ratio between perfusion at the dependent and non-dependent parts. *Paper V* therefore describes how inclusion of a passive arteriolar resistance reduces this ratio towards values similar to those found in the literature.

2.1.3 Blood Model

Oxygen concentration in the blood depends both on the oxygen and carbon dioxide partial pressures because of the Bohr-Haldane effect i.e. competitive binding of O_2 and CO_2 to hemoglobin. In addition the oxygen and carbon dioxide concentrations depend on other properties of the blood, i.e. the concentration of haemoglobins, 2,3-diphospoglycerate and non-bicarbonate buffers. An already developed model of blood acid-base chemistry by Rees and Andreassen [17, 19] is therefore used for calculation of concentrations of oxygen and carbon dioxide in the blood. The blood model also includes a description of the dynamics of O_2 and CO_2 between the arterial and venous blood pool.

2.1.4 Gas-Exchange Model

Paper VI describes gas-exchange in the lungs by incorporating the other sub models. Storage and transport of O_2 and CO_2 between environment, anatomical dead space, alveoli, capillaries, arterial and venous blood are described in details. Flow of air from the environment and into the lungs involves heating and addition of water to the air. Pulmonary gas-exchange is calculated by assuming equilibrium between partial pressures in the alveoli and arterial end of the capillaries. In this way gas-exchange can be calculated by mass balance of the gas concentrations at the venous and arterial end of the capillaries and capillary perfusion. The paper also introduces a simplified model of the mixing of gas within the anatomical dead space.

Chapter 3.

Summary of Papers

As described in chapter 2 the total model of the respiratory system has led to the writing of six papers. The following chapter summarizes all the papers and enhances the main points of the individual papers regarding the answers to the three main research questions stated in chapter 1. Readers are referred to appendix A for the papers in their complete form.

3.1 PAPER I

3.1.1 Aim

The aim of this paper is to build a model that can be used to explore theoretically under which conditions an alveolus will show instability, when subjected to a range of transmural pressures. To investigate this, a model of an alveolus including the effects of surfactant and elastic properties of the alveolar wall is developed.

3.1.2 Methods

The alveoli are modelled as being spherical with an opening consisting of a rigid ring (Figure 3.1). In this way simple geometric formulas can be used to determine radius, surface area and volume of the alveolus.

Alveolar transmural pressure, P_{TM}, is defined as the difference between the pressure inside the alveolus and the extra alveolar hydrostatic pressure exerted by the parenchyma surrounding the alveolus. P_{TM}, is counterbalanced by the mechanical properties of the alveolus i.e. an elastic component due to the alveolar wall, P_E, and a component due to the surface tension of the alveolar air-liquid interface, P_S, as stated in Eq. 2.

$$P_{TM} = P_E + P_S \qquad (2)$$

The model of P_E is based on PV-measurements from excised rabbit lungs inflated with saline [37]. Figure 3.2 shows the data read from Smith and Stamenovic [37] and a fitted empirical model of P_E. PV-measurements by Smith and Stamenovic [37] showed some degree of hysteresis, which has been disregarded in this model.

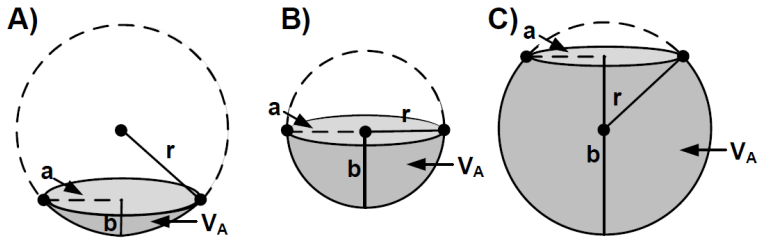

Figure 3.1 Illustration of an alveolus, assuming that the circumference of the alveolar opening is constant. a: alveolar opening radius. r: radius of the alveolus. b: height of the alveolus.

It is assumed that the pressure, P_S, due to the surface tension, γ, of the alveolar air-liquid interface can be calculated from Laplace's law, as stated in *Eq.* 3.

$$P_S = \frac{2\gamma}{r} \quad (3)$$

where r is the radius of the alveolus.

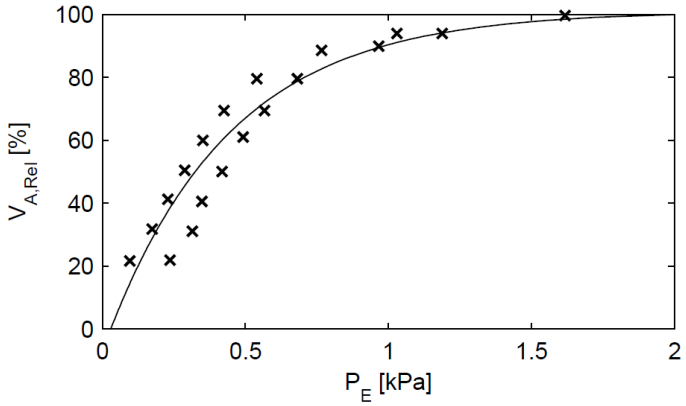

Figure 3.2 The model (curve) of recoil pressure, P_E, exerted by the tissue of an alveolus and the volume of the alveolus. Data (crosses) have been read from Smith and Stamenovic [37].

The model of the surface tension is shown as a function of relative compression of alveolar surface area in Figure 3.3. The figure shows how properties of surfactant impose hysteresis when the alveolar surface area is compressed below 62%.

During the compression starting at "*Start expir1*" the concentration of the surfactant monolayer in the air-liquid interface is increased and the surface tension is reduced accordingly. When surface area has been reduced to 62% of its initial area, the maximal possible surfactant concentration has been reached and the surface tension is constant. When the relative surface area is increased again at "*Start inspir1*" the surface tension rises up to a maximal equilibrium surface tension of 28 mN/m.

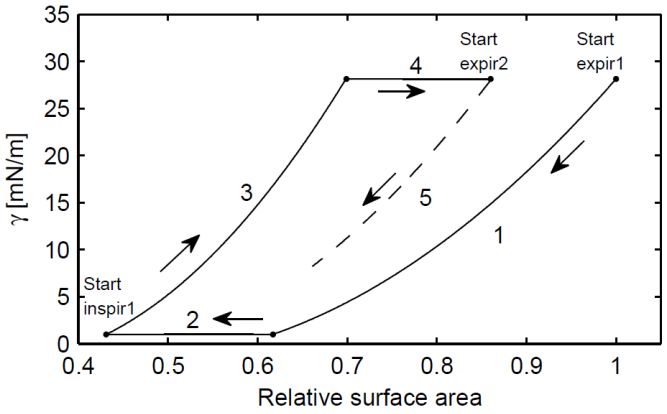

Figure 3.3 Surface tension, γ, as a function of the relative alveolar surface area

In order to determine under which circumstances alveoli show instabilities, model simulations have been performed in five situations: 1) no effect of lung tissue elastic properties and a constant surface tension from a liquid-air interface without surfactant, 2) the effect of lung tissue elastic properties alone, 3) the effect of lung tissue elastic properties and a constant high surface tension from a liquid-air interface without surfactant, 4) the effect of surfactant alone and 5) both the properties of surfactant and tissue elastic properties included. Finally the simulated total *PV*-relationship is compared with data obtained from excised cat lungs. However, in this summary only results from simulation experiments number 1, 3 and 5 will be shown.

3.1.3 Results

Figure 3.4-A shows simulated *PV*-curves for an alveolus without the effects of lung tissue elasticity and a constant surfactant tension equal to surface tension of plasma. Negative slopes of the curves, implies that pressure increases with

decreasing volumes. This is a situation of unstable equilibrium, where at a given pressure any small perturbation of the alveolar volume will either lead to collapse to zero volume or expansion to infinite volume. By increasing the radius of the rigid ring the alveolar *PV*-relationships show some degree of stability for small volumes. However the alveoli will still "pop-open" when pressure reaches a certain level. Figure 3.4-B shows the effect of including the tissue elastic properties. The tissue elasticity stabilizes the alveolus so that when the opening pressure is reached it pops open to a finite volume. When the opening radius is increased to 150 µm the alveolus is stabilized by the tissue elastic properties even without the effects of surfactant.

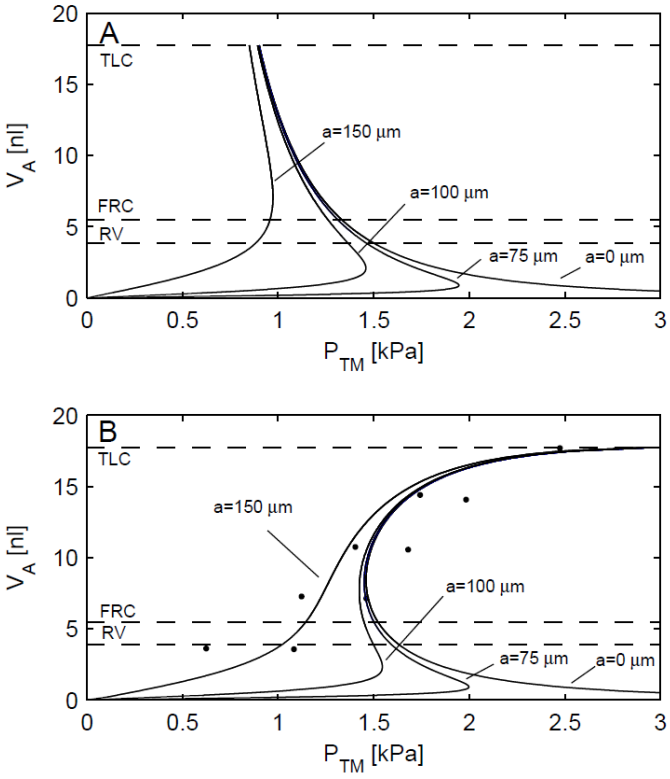

Figure 3.4 A: PV-curves for an alveolus without surfactant and tissue elastic properties. B: Simulations of the alveolar PV-curve including the effects of tissue elastic properties and a surface tension of 73 mN/m. The radius of the rigid ring a, varies between 0 µm, 75 µm, 100 µm and 150 µm. Experimental data indicated by dots [119]. The dashed lines indicate RV, FRC and TLC if all alveoli in the lungs were assumed to be identical.

Figure 3.5 shows simulation results of an alveolus including both properties of surfactant and tissue elasticity. For the geometry where the radius of the rigid ring

is zero, the alveolar *PV*-curve is plotted in Figure 3.5-A. During deflation the alveolus is now completely stable and even deflation from *TLC* (point 1) down to *RV* (point *5*) followed by inflation through points *6, 4* and *1* will keep the alveolus stable. However, if the alveolus is subjected to alveolar pressure below 0.1 kPa, it will close and this closure is irreversible.

If the radius *a* of the rigid ring is 75 µm (Figure 3.5-B), then closure of the alveolus becomes reversible with an opening pressure of 0.8 kPa. In this situation the alveolus will open with a "pop", jumping from the volume at the opening pressure to a higher volume. This is shown in Figure 3.5-B by an arrow with "Pop" noted. A further increase to a = 100 µm will eliminate the ability of the alveolus to pop open and with a = 150 µm the alveolus will be completely stable.

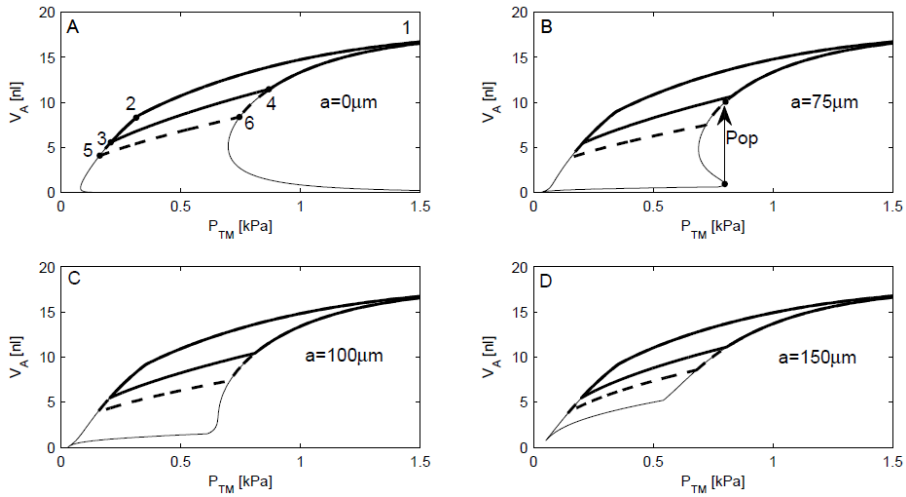

Figure 3.5 The simulated *PV*-relationship of an alveolus including the mechanical properties of the tissue elasticity and surfactant. The bold line is a simulation with alveolar volumes ranging from *TLC to FRC* and back. The bold dashed line represents the physiological range of volume changes from *TLC* to *RV*. The lowermost line shows a simulation of compressions from maximum surface area to 5 %. In B the alveolus will "pop" open, once the transmural pressure exceeds the opening pressure of 0.8 kPa. The alveolar volume will suddenly increase as indicated by the arrow labeled Pop.

3.1.4 Conclusions

The analysis indicates that without surfactant and with a small radius, *a*, of the rigid ring, the alveolus is always at an unstable equilibrium with the capacity to both close irreversibly and to open with infinite volume. By assuming the radius of the rigid ring to be larger than zero, the closing can be made reversible, although a fairly large pressure is required to reopen a collapsed alveolus. A radius of 100 µm seems in agreement with radiograph of the alveoli [120]. Simulations performed

without surfactant, but with the tissue elasticity unaffected shows that the alveoli are stable when the alveolar opening radius is 150 μm, but unstable for opening radii of 0, 75 and 100 μm. Alveolar behavior is stable for radii larger than 100 μm when both surfactant and tissue elasticity are taken into account. Having investigated under which conditions a single alveolus shows instability, the next step is to incorporate this model into a stratified model of the respiratory system and include the effect of chest wall and hydrostatic gradient down the lungs.

3.2 PAPER II

3.2.1 Aim

The aim of this paper is to include the alveolar model developed in *Paper I* in a stratified model of the whole lungs. The paper introduces the effects of the chest wall elasticity and hydrostatic gradient caused by the weight of the lung tissue and blood. Furthermore, the model includes an anatomical description of the cross-sectional area of the lungs derived from *CT*-scans. The model is validated against data found in the literature regarding hysteresis and lung compliance of the static *PV*-curve, change in lung depth and density during tidal breathing and distribution of ventilation in the lungs.

3.2.2 Methods

The paper introduces the concept of the lungs divided into layers distributed from the non-dependent to the dependent part of the lungs, as it was shown conceptually in Figure 2.1. By including the effect of chest wall elasticity, P_{CW}, and hydrostatic gradient, P_{Hydro}, of lung parenchyma, pressure within the alveoli, P_A, can be described by *Eq.* 4.

$$P_A = P_{S,i} + P_{E,i} + P_{CW} + P_{Hydro,i} + P_{Mus} \qquad (4)$$

where i is the index controlling layer depth measured from the non-dependent (i=1) to the dependent part (i=N_{Layers}) of the lungs. P_{Mus} is the pressure generated by respiratory muscles, which is assumed to be zero. The model of the pressure component due to chest wall elasticity is built on experimental data from Konno and Mead [121]. Data read from Konno and Mead [121] are shown with a fitted sigmoid curve for PCW in Figure 3.6.

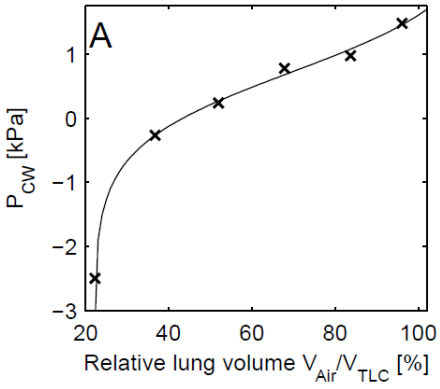

Figure 3.6 The relationship between total lung volume and pressure exerted by chest wall. Data (crosses) read from Konno and Mead [121].

The pressure component due to the hydrostatic gradient is calculated by *Eq.* 5.

$$P_{Hydro,i} = \sum_{j=1}^{i-1} \rho_{Lung,j} \cdot g \cdot t_j \qquad (5)$$

where $\rho_{Lung,j}$ is the density of layer j, g is the gravitational acceleration and t_j is the vertical thickness of layer j. In addition to these components a new model of the tissue elasticity is introduced. The new model (*model II*), assumes that lung tissue to some degree resists collapse, by means of producing a small negative pressure at low lung volumes.

A profile of lung cross-sectional areas, A_{Scan}, as a function of lung depth, D_{Scan}, was constructed from high resolution *CT*-scans taken of a healthy subject in supine position provided and segmented by Lo et al. [122]. During simulation the depth-area curve must be scaled to match the simulated lung volume. This is shown in Figure 3.7-A where the volume of air in the lungs decreases from a volume at *TLC* to a lung volume of 3l. Figure 3.7-B shows the distribution of volume when the lungs are divided into 10 layers ($N_{Layers} = 10$) at *TLC*.

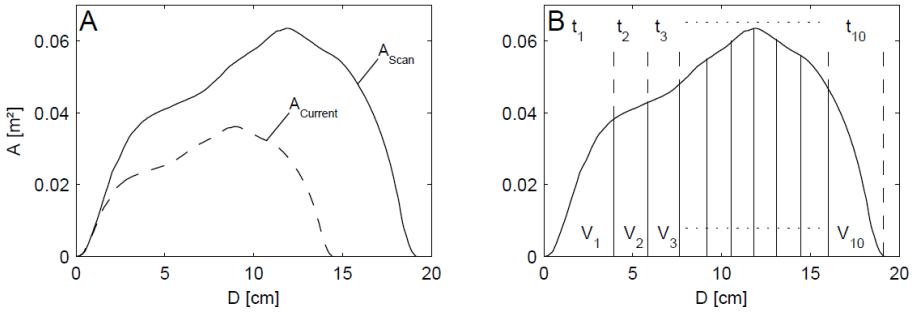

Figure 3.7 A: The relationship between the cross sectional area, A, and lung depth, D, at total lung capacity of 6.8 l (solid line) and at 3 l (dashed line). B: The distribution of volume in layers when the lungs are divided into 10 layers. The thickness, t_i, and volumes, V_i, of each layer are also illustrated.

Different model simulations are performed by varying the alveolar pressure in order to validate the model against experimentally measured hysteresis and lung compliance of the static *PV*-curve, change in lung depth and density during tidal breathing and ventilation distribution down the lungs.

3.2.3 Results

Figure 3.8 shows the mean *PV*-curve in healthy subjects for a study by Sharp et al. [49] and a model simulation with the same alveolar pressure range from 0 to 2.66 kPa. Both simulated hysteresis and compliance are in good agreement with measurements by Sharp et al. [49].

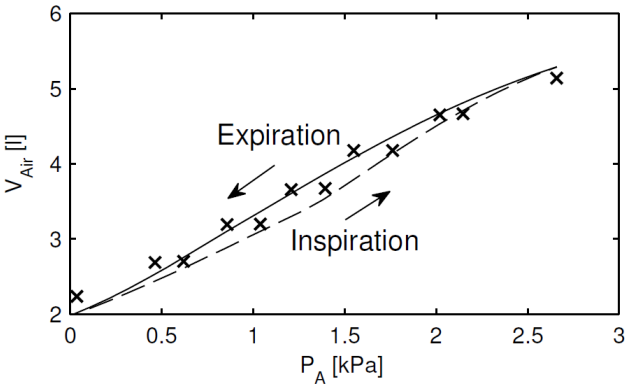

Figure 3.8 The static pressure-volume relationship during a simulation with an alveolar pressure range between 0 and 2.66 kPa. PV-measurements by Sharp et al. [49] (crosses) are also shown. Dashed and solid lines indicate inspiration

Figure 3.9 shows density calculations from a study by Millar and Denison [123] along with simulated density distribution down the lungs at *TLC* and *RV* using the two models of lung tissue elasticity. No difference between the two models is observed at *TLC* and both simulations follow well the homogenous density around 0.1 g/cm^3. However, using *model I* the alveoli collapse at the most dependent layers of the lungs leading to a marked increase in density in these layers. This is not shown in the data by Millar and Denison [123]. The density simulated by using *model II*, however, is in good agreement with measured data. Therefore it is indicated that lung tissue may to some degree resist collapse and *model II* is the most appropriate model to describe density distribution.

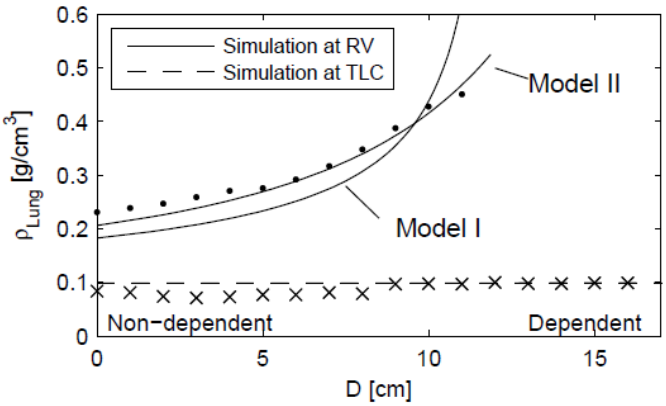

Figure 3.9 Simulated density, ρ_{Lung}, related to lung depth, D, is shown at *TLC* (dashed line) and *RV* (solid line) for both models of the lung tissue elasticity. Data read from Millar and Denison [123] are shown for *TLC* and *RV* (crosses and dots, respectively).

Figure 3.10 shows the simulated ventilation distribution with *models I* and *II* of the lung tissue elasticity along with data read from a study by Brudin et al. [75]. Even though both models imitate the main trend in data, both models underestimate the increase in ventilation from the non-dependent to the dependent part of the lungs, observed by Brudin et al. [75].

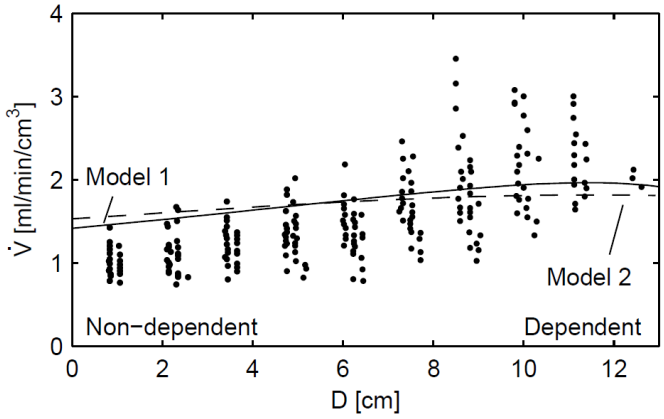

Figure 3.10 Simulation of the ventilation distribution down the lungs using model I (solid line) and model II (dashed line) along with the data read from Brudin et al. [75] (dots) .

3.2.4 Conclusions

The presented model of the whole lung is validated against experimentally measured ventilation distribution, density distribution, lung volumes, *PV*-curve compliance and hysteresis of healthy human subjects in supine posture. Two models of lung tissue elasticity have been developed. According to measurements of density distribution at *RV* it appears that the connecting fibers and tissue exert some negative pressure at very low lung volumes resisting collapse. The model simulates a heterogeneous ventilation distribution down the lungs and indicates no alveolar collapse at *FRC* and *RV*. The model is capable of describing the most important static mechanical properties of the respiratory system, however in order to simulate mechanically ventilated subjects the model should also include important dynamics lung mechanics i.e. airway resistance and viscoelastic properties.

3.3 PAPER III

3.3.1 Aim

The aim of this paper is to combine a model of airway resistance and viscoelastic properties of the lungs with the static ventilation model described in *Paper I* and *II*. The dynamic model parameters are identified from an experimental study performed on five mechanically ventilated healthy subjects without any sedation and anesthetics.

3.3.2 Methods

By including the effect of airway resistance and viscoelastic properties, pressure at the mouth, P_M, is partitioned into the pressure, P_{AW}, overcoming airway resistances, the pressure, P_{St}, to balance the recoiling force from the static compliance, and the pressure, P_{VE}, accounting for the viscoelasticity. The static pressure, P_{St}, is similar to *Eq.* 3, composed of pressures due to: the chest wall, P_{CW}; the hydrostatic effects of the lung tissue and blood, P_{Hydro}; surface tension, P_S; lung tissue elasticity, P_E. The pressure at the mouth can be expressed by *Eq.* 6.

$$P_M = P_{AW} + \underbrace{P_{CW} + P_{Hydro,i} + P_{S,i} + P_{E,i}}_{P_{St,i}} + P_{VE,i} \qquad (6)$$

The pressure drop due to airway resistance can be described using Rohrer's equation as stated in *Eq.* 7 [124].

$$P_{AW} = K_{AW\_1} \cdot \dot{V}_L + K_{AW\_2} \cdot \left|\dot{V}_L\right| \cdot \dot{V}_L \qquad (7)$$

where $\dot{V}_L$ is the total pulmonary ventilation and K_{AW_1} and K_{AW_2} are the constant Rohrer's parameters, describing the laminar flow resistance and turbulent flow resistance, respectively. Alveolar viscoelasticity at layer i has been implemented with parameters describing the viscoelastic capacitance (C_{VE}) and resistance (R_{VE}) in the same way as it was done previously by e.g. Jonson et al. [58] and Ganzert et al. [62] for the whole lung.

An experiment was performed on five healthy subjects to identify the dynamic model parameters (K_{AW_1}, K_{AW_2}, C_{VE} and R_{VE}). The experiment was performed by a large inflation and deflation of the lungs including airway occlusions, similar to the one presented by Zhao et al. [42]. Effects of lung volume and flow on airway resistance and viscoelasticity were during the experiment separated by delivering a fixed volume of 500 ml in six steps at two fixed flow rates. Before the experiment subjects were carefully instructed to relax and not participate in the ventilation because no sedation and anesthetics were given.

3.3.3 Results

Figure 3.11-A shows a typical pressure profile measured by the ventilator from a subject that is participating in the ventilation and is not fully relaxed. Figure 3.11-B shows a pressure profile from the same subject after 5 minutes. Since no ripples are present it is assumed that the subject is fully relaxed.

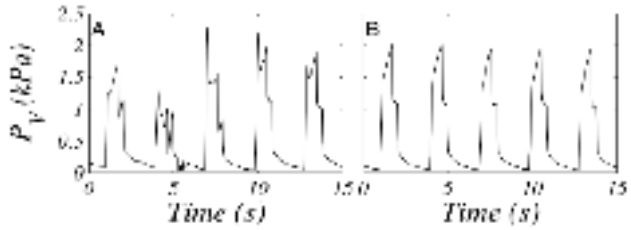

Figure 3.11 Pressure measured by the ventilator, P_V, as a function of time. A: Pressure measurements of a subject participating in the ventilation. B: A fully relaxed subject not participating in the ventilation.

An example of the dynamic *PV*-curve is shown in Figure 3.12. Each of the six inflation steps with two fixed flow rates and six deflation steps can be identified. Due to viscoelastic properties, ventilator circuit and airway resistances it can be identified that the two different inflation rates cause two different pressure drops. The developed dynamic model was capable of reproducing the measured dynamic *PV*-curve with very small error. The static *PV*-points were used to estimate static lung compliance and hysteresis. The mean static compliance between the two extremes was 1.04 ± 0.17. Mean maximum hysteresis being the maximum pressure difference between the static expiratory and inspiratory limbs at equal volumes was 0.084 ± 0.035.

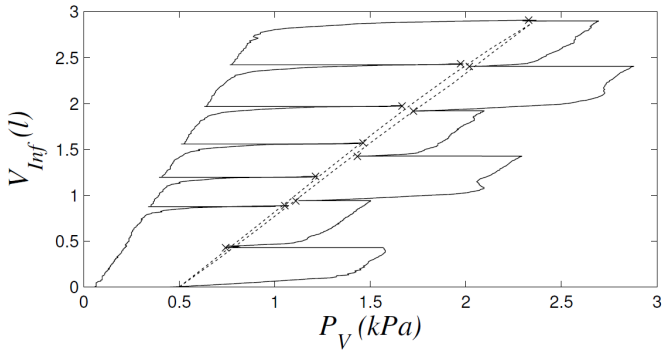

Figure 3.12 Measured pressure-volume relationship from subject number 2. Crosses indicate the measured static pressure-volume points. Dotted line shows a simulated static pressure-volume curve using the identified parameters.

3.3.4 Conclusions

Using the measured ventilator pressure as input, the model was able to reproduce the measured ventilation and volume profiles with small errors. Furthermore, the model simulates the hysteresis and compliance observed in the static *PV*-curve in the healthy subjects. By comparing the pressure profiles measured by the ventilator at the beginning of the experiment with measurements after five minutes, smooth and homogenous profiles in the later of the two indicate that it is possible to measure both static and dynamic lung mechanics without sedation and anesthetics. This paper shows that the developed model is able to describe local ventilation in the lungs during mechanically ventilation by taking into account the most important properties of the respiratory system i.e. lung tissue elasticity, surface tension determined by the effects surfactant, chest wall elasticity, gravity, airway resistance and viscoelastic properties of the lungs. The paper concludes the development of the ventilation model. The next step is to develop a model of the pulmonary perfusion.

3.4 PAPER IV

3.4.1 Aim

The aim of this paper is to describe pulmonary microcirculation mathematically by a stratified model of the lungs, enabling simulation of capillary blood perfusion around the alveoli. The model includes aspects of the capillary geometry, hemodynamics and blood rheology. Model simulations are compared to measurements of the perfusion distribution in the pulmonary microcirculation during mechanical ventilation; total capillary blood perfusion; capillary blood volume; capillary surface area and transition time during different ventilator settings.

3.4.2 Methods

The blood perfusion through a capillary at layer i, conceptual shown in Figure 2.1, can be determined by *Eq.* 8.

$$Q_{Cap,i} = \frac{P_{a,i} - P_{v,i}}{R_{Cap,i}} \qquad (8)$$

where $P_{a,i}$ is the blood pressure proximal to the capillary, $P_{v,i}$ is the venous capillary blood pressure and $R_{Cap,i}$ is the resistance to flow in the capillary at layer *i*.

Capillary transmural pressure is not uniform along the entire length of a capillary and the capillary pressure should decrease along the capillary before finally reaching the venous pressure, $P_{v,i}$. This is approximated by modelling the capillaries in a number of segments, $N_{Segments}$, of equal lengths each accounting for a pressure drop. This is illustrated in Figure 3.13 for a capillary divided into three segments.

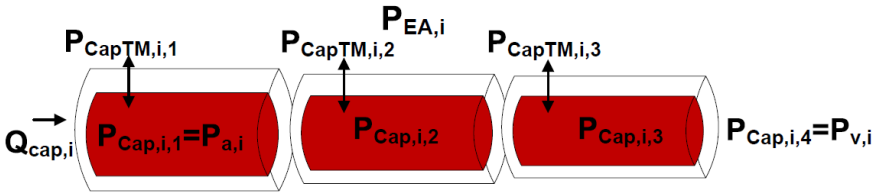

Figure 3.13 Schematic representation of the capillaries divided into three segments each having a pressure drop. P_{EA}: Extraalveolar pressure. P_a and P_v: Arterial and venous blood pressure. Q: Blood perfusion. P_{CapTM}: Capillary transmural pressure. P_{Cap}: Capillary pressure.

Scanning electron micrographs of the alveolar wall reveals a circular capillary cross-section under positive transmural pressures, but under negative transmural pressures the capillaries flattens. A modified version of Poiseuille's law stated in

Eq. 9 is therefore used to calculate capillary resistance, $R_{Cap,i,n}$, at segment n for elliptic capillaries at negative transmural pressures [125].

$$R_{Cap,i,n} = \frac{0.75 \cdot L_{Cap} \cdot \eta_{Blood}(r_{2,i,n})}{r_{1,i,n} \cdot (2 \cdot r_{2,i,n})^3 \cdot M_o} \qquad (9)$$

where L_{Cap} is the length of a capillary, η_{Blood} is the blood viscosity calculated from the model by Pries et al. [71] shown in Figure 1.7, $r_{1,i,n}$ and $r_{2,i,n}$ are the radii describing the shape of the elliptic capillaries and M_0 is a correction factor.

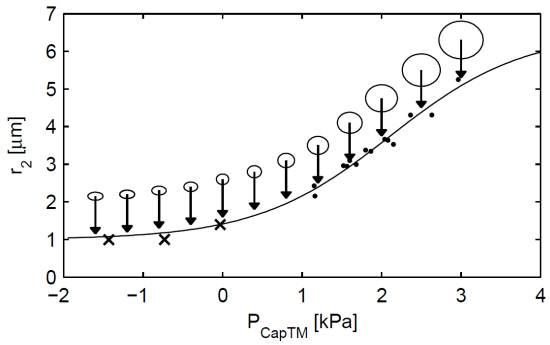

Figure 3.14 The relationship between capillary transmural pressure and capillary radius. Data read from Sobin et al. [126] (dots) and Glazier et al. [127] (crosses) are illustrated. A sigmoidal curve has been fitted to the data points. The shapes of the capillaries are indicated at different transmural pressures.

Figure 3.14 shows observation of capillary dimensions under different transmural pressures performed by Sobin et al. [126] and Glazier et al. [127] along with an empirical fitted curve of the radius, $r_{2,i,n}$, as a function of capillary transmural pressure.

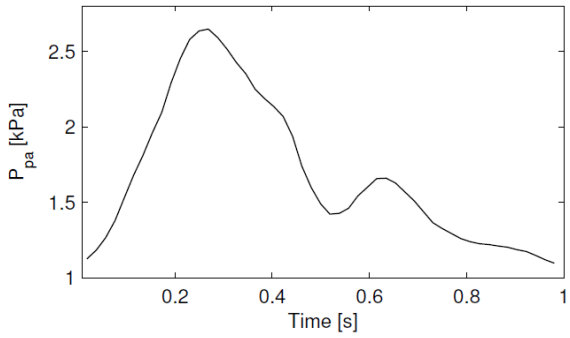

Figure 3.15 The pulmonary pressure proximal to the capillaries at the height of the pulmonary valve, P_{pa}. The profile is shown for one heartbeat [128] scaled into the pressure range for pulmonary capillaries [61, 67].

The pressure proximal to the capillaries was estimated by scaling a pressure profile measured in the pulmonary artery [128] to a pressure range between 1-2.7 kPa with a mean of 1.73 kPa [61, 67] (Figure 3.15).

3.4.3 Results

The simulated distribution of mean capillary perfusion at different lung depths during tidal breathing is shown in Figure 3.16 against measured data read from Brudin et al. [74]. It can be seen that the model is capable of imitating the major trend in data, however, the perfusion at the top of the lungs is underestimated, which causes a too high ratio between dependent/non-dependent perfusion. Furthermore, the reduced perfusion in the dependent part (*zone IV*) of the lungs, shown by others [73, 83, 129, 130], is not simulated.

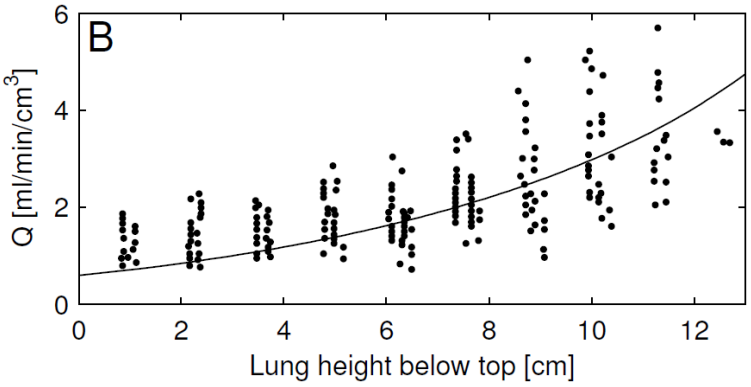

Figure 3.16 Simulation of the perfusion (solid line) calculated as ml per minute per cm^3 lung parenchyma (including air) along with data read from Brudin et al. [74] (dots).

Figure 3.17-A shows the pulmonary capillary transition times, TT_{Cap}, for layers number 1, 25, 50, 75 and 100. The mean transition times are plotted against lung depth in Figure 3.17-B. The simulation shows a highly pulsatile and heterogeneous distribution of the transition time, with a mean range from 2.2 to 10.9 seconds (dependent to non-dependent). In good agreement with transition time estimated in the literature [131-135].

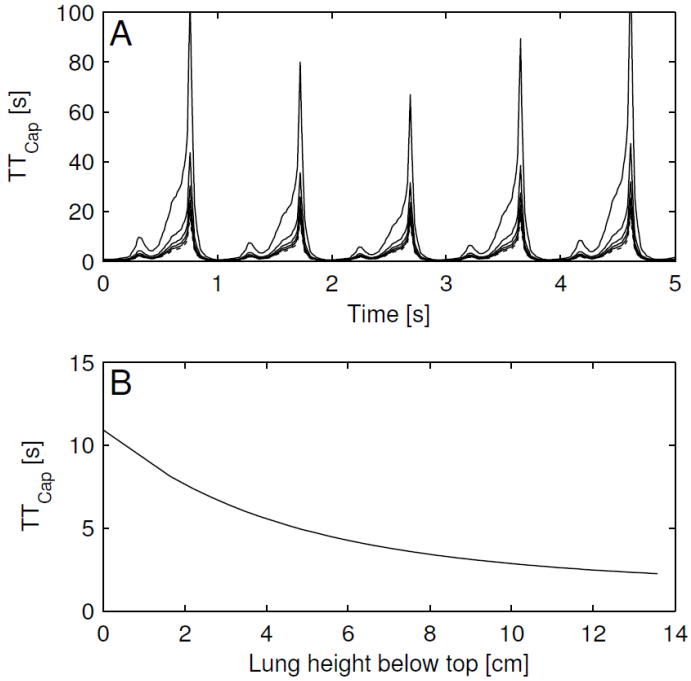

Figure 3.17 A: Transition time during a tidal breath in layer number 1, 25, 50, 75 and 100 (most dependent, dashed line) and B: Mean transition time as a function of the lung depth.

3.4.4 Conclusions

The developed model of pulmonary capillary perfusion that links perfusion with lung mechanics in a stratified model is capable of simulating the effect of gravity upon distribution of the pulmonary perfusion. Even though the reduced perfusion at the dependent part (*zone IV*) of the lungs is not simulated, the model is in agreement with experimentally measured data of the total capillary perfusion, total capillary blood volume, total capillary surface area and transition time of the red blood cells passing the pulmonary capillary network. The simulated ratio between dependent/non-dependent perfusion was, however, overestimated therefore another physiological component that can lower this ratio between the perfusion in the dependent and non-dependent part of the lungs is needed. As *Paper V* will show, this component is a constant and uniformed distributed arteriolar resistance.

3.5 PAPER V

3.5.1 Aim

The aim of this paper is to reduce the simulated ratio between dependent/non-dependent perfusion. As described in chapter 1 arteriolar resistance accounts for a pressure drop similar to the one caused by the capillary network. Hence, this paper investigate to which extend inclusion of a constant pulmonary arteriolar resistance in the model of pulmonary perfusion described in *Paper IV* improves the ratio between dependent/non-dependent perfusion.

3.5.2 Methods

Figure 3.18 shows a modification of Figure 3.13 i.e. a conceptional drawing of the perfusion model with a constant arteriolar resistance and the capillary segments.

By including an arteriolar resistance the perfusion through an arteriole and a capillary, Q_i, at layer i can be determined by *Eq.* 10.

$$Q_i = \frac{P_{Art,i} - P_{v,i}}{R_{Art} + R_{Cap,i}} \qquad (10)$$

where $P_{Art,i}$ is the arterial blood pressure, $P_{v,i}$ is the venous capillary blood pressure, R_{Art} and $R_{Cap,i}$ is the resistance to flow in the arteriole and capillary at layer i. In order to explore the effect of an arteriolar resistance on the ratio between dependent/non-dependent parts of the lungs, a sensitivity analysis with four different arteriolar resistances was performed.

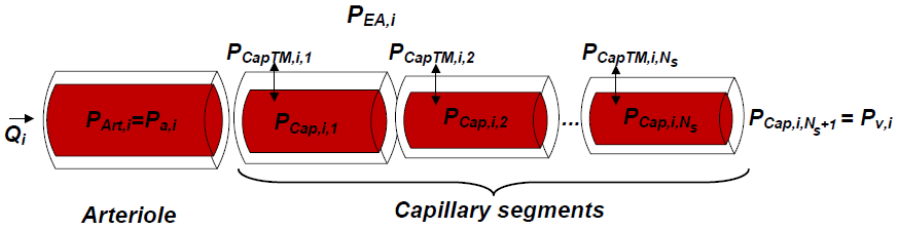

Figure 3.18 Schematic representation of an arteriole and a capillary divided into segments each having a pressure drop. $P_{EA,i}$: Extraalveolar pressure. $P_{a,i}$: Arterial blood pressure. $P_{v,i}$: Venous blood pressure. Q_i: Blood perfusion. $P_{CapTM,,i}$: Capillary transmural pressure. $P_{Cap,i,n}$: Capillary pressure at layer i and segment n. $P_{Art,i}$: Arteriolar pressure.

3.5.3 Results

Figure 3.19 shows results from the sensitivity analysis of the arteriolar resistance on the distribution of perfusion down the lungs.

The figure includes a simulation similar to the one described in *Paper IV* (bold line). As shown this simulation underestimated the perfusion in the non-dependent part of the lungs compared to data from the study by Brudin et al. [74] and the perfusion ratio between dependent/non-dependent part of the lungs was 11.2. In the data from Brudin et al. [74] the ratio is about 3.0, determined from a second order polynomial fit to the data. Since the pulmonary input blood pressure is the same for all simulations, simulation with a low arteriolar resistance of 0.1 kPa · s/nl overestimates the perfusion measured by Brudin et al. [74]. Simulation with a high arteriolar resistance of 1.0 kPa · s/nl on the other hand reduces perfusion so much that the data by Brudin et al. [74] is underestimated.

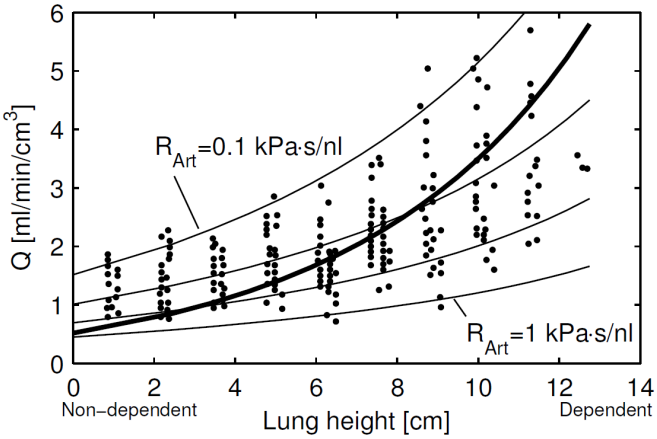

Figure 3.19 Simulation results of the sensitivity analysis on R_{Art}. Perfusion distribution is shown as a function of lung height. Thick line shows simulation similar to one described in Figure 3.16 Indicated on the figure are simulation results of arteriolar resistances of 0.1 kPa · s/nl and 1 kPa · s/nl. In between are simulation results of arteriolar resistances of 0.25 kPa · s/nl and 0.5 kPa · s/nl. Data are from Brudin et al. [74] (dots).

The pressure drop caused by arterioles was here assumed to be 0.53 kPa. This was simulated for an arteriolar resistance R_{Art} = 0.5 kPa · s/nl. This value of arteriolar resistance gives a perfusion ratio of 4.0 and although this remains higher than the experimentally observed ratio of 3.0 the results indicate that including an arteriolar resistance significantly improves the capability of the model to fit measured perfusion distributions. The fit to experimental data could be further improved by modifying the number of capillaries per alveolus or the length of capillaries both of which are model parameters resulting in scaling of the perfusion distribution curves.

3.5.4 Conclusions

Model simulation with arteriolar resistance reduced the perfusion ratio between dependent/non-dependent and improves the ratio to 4.0 using a resistance of 0.5 kPa·s/nl. This leaves room for other mechanisms, either passive (anatomical) or active (hypoxic vasoconstriction) to further reduce this ratio. Before concluding that other mechanisms must be included in the model it is interestingly to see the effects on the respiratory system and the gas-exchange. The next paper will combine the ventilation model described in *Paper I-III*, the perfusion model described in *Paper IV-V* with a previous model of blood acid/base chemistry by Rees and Andreassen [17, 19]. This combined model of the respiratory system is then used to investigate the effects of gravity on the respiratory gas-exchange.

3.6 PAPER VI

3.6.1 Aim

The aim of this paper is to investigate the effect of gravity on the respiratory system and pulmonary gas-exchange. The investigating is performed with a stratified model describing storage and transport of CO_2 and O_2 in the environment, anatomical dead space, alveoli, capillaries, arterial and mixed venous blood. The model incorporates the previous models of the pulmonary ventilation and perfusion described in *Paper I-V*. The model is expanded with a physiological description of the pulmonary gas-exchange similar to the one presented by Poulsen et al. [136]. Also the acid-base chemistry of the blood is included in the model [17, 19]. Furthermore, equations are added in order to describe the mixing of air in the anatomical dead space.

3.6.2 Methods

Figure 2.1 in chapter 1 showed the conceptual drawing of the total tidal breathing model describing flow of O_2 and CO_2 between six compartments: environment, *E,* anatomical dead space, *AD,* alveoli, *A,* capillaries, c*,* arterial blood, *a*, and mixed venous blood, *v.* The model describes the lungs as divided into layers distributed from the non-dependent, (i=1) to the dependent part of the lungs (i=N_{Layers}) similar to the structure described in *Paper II-V*.

In order to make model simulations comparable with data found in the literature of quiet voluntarily breathing subjects the model described in *Paper I-V* is modified. Instead of using the pressure exerted by the ventilator as input to the model, the pressure at the mouth is kept constant at barometric pressure (101.3 kPa) and pressure exerted by the respiratory muscles is used as the driving variable of the model.

The anatomical dead space is modelled as a straight pipe divided into a number of longitudinal and radial segments. During simulation of a time step, the model moves air between environment and alveoli by shifting the gas either towards the alveoli or the environment according to the radial distribution of flow velocities.

A simulation of a subject in supine position is used to investigation of the model's capability of describing ventilation, perfusion and gas exchange of healthy subjects. In addition a simulation of a subject exposed to zero gravity and a subject in upright position are used to investigate gravity's effect on the respiratory system and gas exchange. In order to make the three simulations comparable the overall minute ventilation and perfusion were maintained by adjusting peak pressure exerted by the respiratory muscles and systolic/diastolic pulmonary arterial pressure.

3.6.3 Results

The model is validated against a number of measured values found in the literature from supine and quiet voluntarily breathing subject regarding: regional ventilation-perfusion distribution, end-tidal partial pressures, arterial and mixed venous partial pressures of O_2 and CO_2, and arterial and mixed venous oxygen saturations.

Figure 3.20 shows simulated distributions of ventilation and perfusion for a quiet voluntarily breathing subject (full line) calculated as ml/min/cm^3 lung parenchyma (including air).

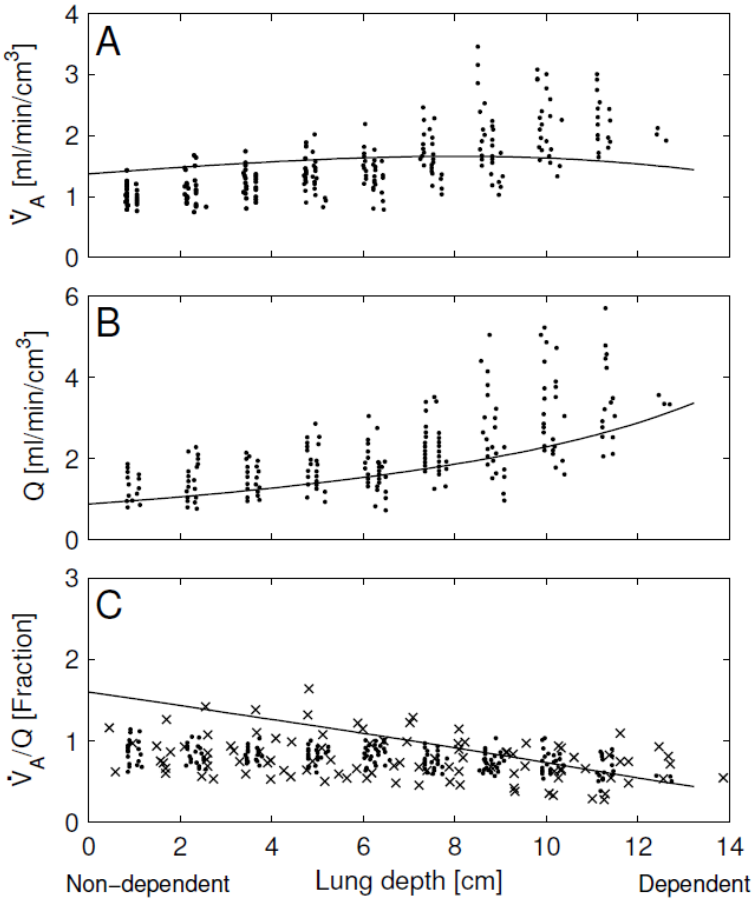

Figure 3.20 Simulated alveolar ventilation calculated per cm3 lung tissue (line) for a subject in the supine position and data measured by Brudin et al. [74] (dots). B: Simulated perfusion per cm3 lung parenchyma (line) and data measured by Brudin et al. [74] (dots). C: Simulated ventilation-perfusion distribution according to lung depth and data measured by Brudin et al. [74] (dots) and Rhodes et al. [76] (crosses).

The number of alveoli and capillaries per cm^3 lung parenchyma increases by a factor of 2.2 from the non-dependent (i =1) to the most dependent layer (i = 20). So even though the ratio of ventilation between the dependent and non-dependent layers is 0.47 meaning that ventilation per alveolus is lowest in the dependent part of the lungs, the ventilation per cm^3 lung parenchyma becomes almost uniform (Figure 3.20-A). PET scan data from Brudin et al. [74] are shown for comparison. Apparently the model underestimates the experimentally determined increase in ventilation with lung depth. Figure 3.20-B shows that perfusion increases from the top towards the bottom of the lungs both due to the effect of gravity and the increasing number of capillaries per cm^3 lung parenchyma at the bottom. The simulated ratio of perfusion per cm^3 between the dependent and the non-dependent part of the lungs Q_{20}/Q_1 is 3.9. This is in good agreement with the ratio in the experimental data by Brudin et al. [74] (Figure 3.20-B).

Simulated $\dot{V}/Q$ -distribution is shown in Figure 3.20-C (full line) along with PET scans from Brudin et al. [74] and Rhodes et al. [76]. The simulated $\dot{V}_A/Q$ -distribution decreases by a factor of 3.6 from 1.6 in the non-dependent part of the lungs to 0.4 in the dependent part of the lungs. This is in contrast to the $\dot{V}_A/Q$ -ratios measured by Brudin et al. [74] and Rhodes et al. [76] which was almost independent of lung depth.

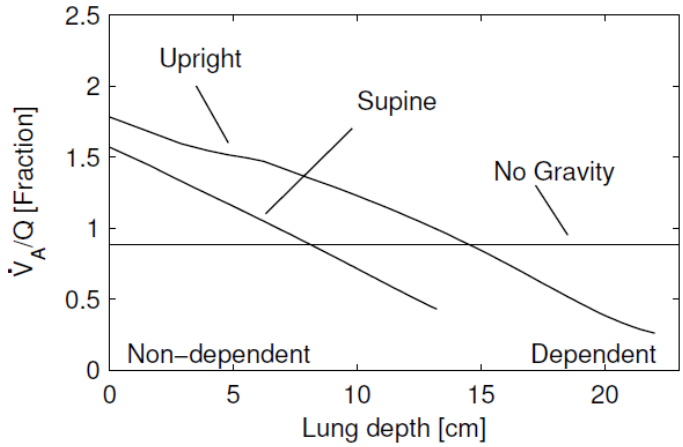

Figure 3.21 Simulation results of ventilation-perfusion distribution down the lungs for a subject in upright, supine and with no gravity.

The effect of gravity on the respiratory system is investigated with a simulation of subject in upright, supine and exposed to no gravity. Figure 3.21 shows the simulated $\dot{V}_A/Q$ -distributions down the lungs for the three simulations. The simulated mean lung height in upright position was 21.2 cm compared to a mean lung height of 12.8 cm for the subject in supine position. As a result of larger

lung height in upright position the effect of gravity also increases the difference between $\dot{V}_A / Q$ -ratio at the top and bottom of the lungs. The $\dot{V}_A / Q$ -ratio for the simulated subject exposed to no gravity is represented as straight line independent of lung height.

Table 3.1 shows the mean values of alveolar, arterial and mixed venous O2 and CO2 contents for the three simulations along with values found in the literature. As a measure of the extent to which gravity compromises the gas exchange properties of the lungs we use the pressure difference of O_2 and CO_2 between end-tidal and arterial blood, $P_{ET}O_2$-P_aO_2 and P_aCO_2-$P_{ET}CO_2$.

Table 3.1 Simulation results of the effect of gravity in the alveoli, arterial and venous blood. Included in the table are mean results from simulation of a subject in supine and upright position along with the mean results with no gravitational distribution. For comparison values found in the literature are also included.

	Alveoli						**Arterial**			**Venous**			**Gas exchange**	
	P_AO_2 (kPa)			P_ACO_2 (kPa)			P_aO_2 (kPa)	P_aCO_2 (kPa)	s_aO_2 (%)	P_vO_2 (kPa)	P_vCO_2 (kPa)	s_vO_2 (%)	$P_{ET}O_2$-P_aO_2 (kPa)	P_aCO_2-$P_{ET}CO_2$ (kPa)
	Non. Dep	Dep.	End-tidal	Non. Dep	Dep.	End-tidal								
Supine	15.7	10.3	13.9	4.6	5.7	5.1	12.0	5.3	96.9	5.4	5.9	74.7	1.8	0.2
No G.	13.5	13.5	13.6	5.2	5.2	5.1	12.6	5.2	97.2	5.4	5.8	75.1	1.0	0.1
Uprig.	16.1	8.2	14.3	4.5	5.9	5.1	11.0	5.4	96.0	5.3	6.0	73.7	3.2	0.3
Lit.			13.6 [137]			5.1 [137]	12.1 [61] - 12.8 [137]	5.0 [137] - 5.3 [61, 67]	97.0 [138]	5.1 [138] - 5.3 [67]	5.6 [138] - 6.1 [61, 67]	71.0 [138] - 75.0 [67]	0.8 [137] - 2.0 [139]	0.2 [140] - 0.3 [137]

As stated in Table 3.1 results showed that for a normal healthy subject in zero gravity the gas exchange was largely normal, except that the difference P_aCO_2-$P_{ET}CO_2$ is improved from 0.2 kPa to 0.1 kPa, which is slightly better than normal. For a supine subject gas exchange was also normal, except for P_aO_2 = 12.0 kPa being a bit below normal, indicating slightly impaired gas exchange. For an upright subject both the arterial saturation S_aO_2 = 96.0 % and partial pressure P_aO_2 = 11.0 kPa are below normal and the end-tidal to arterial difference, $P_{ET}O_2$-P_aO_2, is increased to 3.2 kPa, which is higher than normal, all indicating compromised gas exchange.

The conclusion is therefore that, according to the model, gravity by itself compromises gas exchange in the upright position, beyond what is seen experimentally.

3.6.4 Conclusions

The developed model of the respiratory system simulates the CO_2 and O_2 storage and transport in the respiratory system of resting healthy person. The model was capable of reproducing physiological parameters measured in supine position, e.g. expired partial pressure, distribution of ventilation and perfusion down the lungs, saturations and partial pressure of the venous and arterial blood. Simulations of

normal ventilation in supine position gave results in good agreement with those found in the literature. Only $\dot{V}_A / Q$-distribution and arterial partial pressures were in supine position simulated just outside the values found in the literature. The model was used to investigate how gravity influences the respiratory system by simulating a subject exposed to zero gravity and a subject in upright position. The results showed that S_aO_2 and P_aO_2 were the parameters that were affected the most by gravity. By including the effects of gravity the model simulated an oxygenation and partial pressure of the arterial blood outside the normal range reported in the literature especially in the upright position where the simulation showed arterial partial pressure of 11.0 kPa, arterial saturation of 96.0 % and pressure difference of O_2 between end-tidal and arterial blood of 3.22 kPa. This indicates that passive or active mechanisms should be included to counteract the effect of gravity.

Chapter 4.

Discussion and Conclusions

Patients with severe lung injuries in the ICU require mechanical ventilation. Appropriate ventilator settings reduce mortality associated with mechanical ventilation. Finding these settings is, however, a compromise of conflicting goals. It is important to secure sufficient oxygenation of the patients, but at the other hand excessive use of pressure, tidal volumes and F_iO_2 to achieve this may cause VILI. Currently this complex task of finding appropriate ventilator settings has not been fully understood e.g. [4, 8, 11-16]. There is therefore a need for a better physiological understanding of the effect of mechanical ventilation on the respiratory system. It needs to be clarified how the mechanical properties of the lungs, local distribution of ventilation, perfusion and gas-exchange are affected by mechanical ventilation. In addition, it has not been fully understood to which extend alveoli are recruited (opens) and derecruited (collapses) during normal tidal breathing. Furthermore, it has not been determined how and to which extent passive or active mechanisms interact with gravity and how they influence the regional distribution of ventilation, perfusion and gas-exchange.

Physiological mathematical models may be a way to explore and clarify these uncertainties and complex connections that may be difficult to investigate experimentally. The overall aim of this PhD-project was therefore to develop a physiological mathematical model that could improve our physiological understanding of the respiratory system. The model developed of the respiratory system describes distributions of ventilation, perfusion and gas-exchange in lungs of a healthy human subject during mechanical ventilation. The model was used to investigate how alveoli behave during breathing and how gravity affects the respiratory system. In chapter 1 the aim of the PhD-project was summarized in three research questions. In the following sections the answers to these three questions will be discussed based on the results presented in the six papers. Furthermore, this chapter will discuss the limitations of the model and necessary future work including a short clinical perspective.

4.1 MAJOR FINDING OF THE THESIS

4.1.1 Total Model of the Respiratory System

A novel comprehensive stratified model of the healthy human lungs has been developed. The model is composed of four sub models, i.e. a ventilation model, a perfusion model, a blood model and a gas-exchange model. The ventilation model describes lung mechanics regarding the lung tissue elasticity, surface tension determined by surfactant, chest wall elasticity, gravity, airway resistance and viscoelastic properties of the lungs. The perfusion model includes a description of the pressure in the pulmonary vessels, the effect of gravity and pulmonary resistance determined by viscosity of blood and the number, length and radius of the blood vessels. Furthermore, the perfusion model includes a distribution of the capillary compliance and arteriolar resistance. The blood model describes the acid/base chemistry of the blood including the Bohr-Haldane effect. The gas-exchange model incorporating the other sub models and describes the storage and transport of O_2 and CO_2 between environment, anatomical dead space, alveoli, capillaries, arterial and venous blood. Each of the sub models is based on physiological assumptions and despite they are founded on measurements from many different studies they are capable of reproducing experimental data from the literature e.g. *PV*-curves, distribution of lung density, ventilation and perfusion, total capillary perfusion, capillary transition time of the red blood cells, arterial, mixed venous and end-tidal partial pressures of O_2 and CO_2.

The model developed of the respiratory system uses pressure exerted by the ventilator as input and is able to simulate the effects of mechanical ventilation on the entire respiratory system. The following sections will discuss what can be learnt from the model regarding stability of the alveoli and the effect of gravity on the respiratory system.

4.1.2 Stability of the Alveoli during Breathing

The conditions under which single excised alveoli show instability were investigated in *Paper I*. The main finding was that the alveolus was stable when properties of both surfactant and tissue elasticity for a healthy subject are taken into account. The alveolar model was incorporated into a stratified model of the entire respiratory system in *Paper II*. Here a new model of tissue elasticity (*model II*) was introduced and compared to the elasticity model presented in *Paper I* (*model I*). The new model assumes that lung tissue to some degree resists collapse, by producing a small negative transmural pressure at low lung volumes. Simulations described in *Paper II* showed that the hydrostatic pressure gradient induces an alveolar volume and density gradient down the lungs. Figure 3.9 shows comparison of measured and simulated density distribution down the lungs using the two lung tissue elasticity models. As indicated in Figure 3.9 *model I* simulates alveolar collapse at *RV*. The collapse of the most dependent layers leads to a marked increase in density in these layers, which is not shown in the data. The

density simulated by using *model II*, however, does not show alveolar collapse and is in good agreement with data. It is therefore indicated that alveoli do not collapse in the healthy lungs because connecting fibers and tissue to some degree resist collapse.

Other mathematical models in the literature have previously simulated hysteresis based on opening and closing of the alveoli e.g. [32, 141, 142]. In these models the effect of surfactant is neglected and hysteresis is a result of recruiting previously closed alveoli. Alveoli simulated in this thesis do not collapse and the simulated hysteresis is mainly a result of the hysteresis of surfactant.

4.1.3 The Effect of Gravity on the Respiratory System

Paper VI investigates the effects of gravity on the respiratory system, which has been widely discussed in the literature e.g. [43, 93-95, 143-146]. The main aim of *Paper VI* was to clarify to which extent gravity alone influences the ventilation, perfusion and gas-exchange distribution down the lungs. In this way it could be elucidated to which extent other mechanisms are responsible for the distribution of blood and air in the lungs. Because simulated lungs in upright position were unable to sustain sufficient oxygenation of the arterial blood and gas-exchange expressed as the pressure difference of O_2 and CO_2 between end-tidal and arterial blood was compromised, it was concluded that there must be other mechanisms counteracts the effects of gravity. It needs further investigations to conclude how and whether passive anatomical gradients [84, 87, 147, 148] or active mechanisms such as hypoxic or hypercapnic pulmonary vasoconstriction [88-90] and bronchodilation [91] participate in the redistribution of air and blood in the lungs.

4.2 MODEL LIMITATIONS AND FUTURE WORK

The development of mathematical physiological models introduces a number of assumptions and simplifications. The assumptions and limitations for this *PhD*-project are discussed in the following.

4.2.1 Surfactant Model

The properties of surfactant described in *Paper I* and *Paper II* are based on the rate of compression defined by the surface area from the study by Lu et al. [149]. However the speed of compression [150] and surfactant composition [151] have also proven to be important aspects [152]. Lu et al. [149] used dynamic cycles lasting 25 seconds per cycle, while human breathing at rest is 12-16 breaths per minute [67] corresponding to 5-3.75 seconds per cycle. Furthermore Lu et al. [149] performed experiments with bovine surfactant. More experimental research regarding surfactant function under the influence of compression ratio, speed of compression and surfactant composition is required for validation of the surfactant model. In this context the model of the viscoelastic properties presented in *Paper*

III also need further investigation. It is not clear whether the viscoelastic properties of the lungs are due to stress adaption in the lung tissue alone, a result of the mechanical behavior of surfactant or something else.

4.2.2 Alveolar Ducts

The finding that alveoli may not collapse in the healthy lungs might be interpreted with some cautions. It has been discussed in the literature whether the surface area of the alveoli changes during quiet breathing [153, 154]. In a model by developed by Wilson et al. [155-157] the surface area of the alveoli is allowed to change without changing the lung volume since the volume in the alveolar ducts are assumed to change depending on surface tension. The alveolar ducts are not included in the present model and the alveolar surface area and volume are in this study assumed to be directly linked through the alveolar radius. Furthermore, the assumption of a rigid ring at the opening of the alveoli still needs further investigation. In a model by Kitaoka et al. [158] the opening radius was modelled as changing with the alveolar volume. In this way it is possible for the alveoli to close and be unventilated without collapsing. The moderate lung densities in the dependent part of the lungs observed by Millar and Denison [123] might therefore be explained by air trapping in closed but not collapsed alveoli. However, it is still not clear in which way the alveoli may close or collapse and in which way the alveolar duct and opening are participating in resisting collapse at very low lung volumes. How they generally affect the lung mechanics is therefore a topic for future investigations.

4.2.3 Heart Function and Passive Pulmonary Resistance

The capillary blood flow in the model of the blood perfusion was estimated at rest. During mechanical ventilation at high pressures, the perfusion is diminished due to the increasing extra alveolar pressure within the lung parenchyma restricting the capillary radius, as seen in *Paper IV*. The cardiac output can be increased from 5-6 l/min at rest to a maximum of 25 l/min during exercise [67]. In response to epinephrine and norepinephrine the heart can increase the isovolumic pressure peaks and hence pump against increased airway pressure levels [67]. The heart could be expected to increase the output in response to constriction of the blood flow in order to improve gas-exchange. Integrating changes in the heart function during mechanical ventilation in the presented model would enable more physiological simulations of changes in the $\dot{V}/Q$ -ratio when the *PEEP* level is raised. This could be of clinical interest according to the problem of avoiding lung edema by means of *PEEP* while maintaining adequate gas-exchange.

4.2.4 Anatomical Gradient and the Anatomical Dead Space

The developed model of the respiratory system does not include parameters that describe the heterogeneity of ventilation and perfusion within the same vertical lung depth, which has previously been reported with high spatial resolution imaging methods (e.g. *SPECT* [80, 81], *PET* [82], *HRCT* [83], microspheres [84, 85]). Alveoli close to the hilum of the lungs tend to be better ventilated and perfused and such differences can of course not be explained by gravity, but may be explained by the anatomy of the pulmonary vascular and airway trees [84, 87]. This might also contribute to the relatively low perfusion observed at the top and bottom of the lungs [73]. Additional contributions to regional differences may arise from for example a ventral-dorsal gradient in the properties of the lung parenchyma, as has been shown in quadruped animals independent of body position [84, 159, 160]. It is also possible that mechanical dilation of vessels situated in the corners between alveoli may increase perfusion in the non-dependent parts of the lungs [147, 148]. The anatomical gradients can not be described with the current model and should be included in the future.

The mixing of air within the anatomical dead space is not only determined by the turbulence as it is assumed in the current model, also diffusion, distance and anatomy of the upper airways all play an role in gas mixing [161]. Especially the anatomical distances from the mouth to the layers at the dependent and non-dependent part of the lungs (here assumed identical) are important for e.g. the end-tidal partial pressure of O_2 and CO_2.

4.2.5 Clinical Perspective of the Model

The presented lung model provides a tool for estimating many parameters that may have both clinical and physiological relevance. The model assists in the understanding of lung function and the effect of different treatments with mechanical ventilation. However, to complete the model it will be necessary to add passive or active mechanisms, which counteracts the effects of gravity. Given such a model, capable of describing gas-exchange in the healthy lungs, the model can be used to study how tidal volume and *PEEP* affect the distribution of ventilation, perfusion and gas-exchange [162]. The model can also be applied to the injured lungs. The model could be used to study how lung edema develops, how fluid distributes in the lungs and how the presence of fluid and proteins compromises the function of surfactant.

4.3 GENERAL CONCLUSIONS

1. A comprehensive stratified physiological model of the total respiratory system has been developed. The model is composed of four sub models, i.e. a ventilation model, a perfusion model, a blood model and a gas-exchange model. The model is able to reproduce physiological data observed in the literature, of e.g. *PV*-curves, distribution of lung density, ventilation and perfusion, total capillary perfusion, capillary transition time of the red blood cells, arterial, mixed venous and end-tidal partial pressures of O_2 and CO_2.

2. Simulated and experimentally measured lung densities indicate that alveoli do not collapse in the healthy lungs and that the hysteresis of the *PV*-curves is mainly due to the hysteresis of surfactant and not to recruitment of alveoli.

3. The simulated lungs were unable to sustain sufficient oxygenation of the arterial blood in upright position, it is therefore concluded that other mechanisms counteract the effects of gravity.

References

[1] M.L. Mogensen, K.L. Steimle, D.S. Karbing and S. Andreassen, A Mathematical Physiological Model of the Pulmonary Capillary Perfusion, *7th IFAC Symposium on Modelling and Control in Biomedical Systems (including Biological Systems)* August 12-14th, Aalborg, Denmark (2009)

[2] K.L. Steimle, M.L. Mogensen, D.S. Karbing, B.W. Smith, O. Vacek and S. Andreassen, A Mathematical Physiological Model of the Pulmonary Ventilation, *7th IFAC Symposium on Modelling and Control in Biomedical Systems (including Biological Systems)* August 12-14th, Aalborg, Denmark (2009)

[3] M.J. Tobin, A. Jubran and F. Laghi, Patient-ventilator interaction, *Am J Respir Crit Care Med* 163 (5) (2001) 1059-1063.

[4] D. Fenstermacher and D. Hong, Mechanical ventilation: what have we learned?, *Crit Care Nurs Q* 27 (3) (2004) 258-294.

[5] ARDSNet, Ventilation with lower tidal volumes as compared with traditional tidal volumes for acute lung injury and the acute respiratory distress syndrome, *N Engl J Med* 342 (2000) 1301-1308.

[6] K.G. Hickling, J. Walsh, S. Henderson and R. Jackson, Low mortality rate in adult respiratory distress syndrome using low-volume, pressure-limited ventilation with permissive hypercapnia: a prospective study, *Crit Care Med* 22 (10) (1994) 1568-1578.

[7] M.B. Amato, C.S. Barbas, D.M. Medeiros, R.B. Magaldi, G.P. Schettino, G. Lorenzi-Filho, R.A. Kairalla, D. Deheinzelin, C. Munoz, R. Oliveira, T.Y. Takagaki and C.R. Carvalho, Effect of a protective-ventilation strategy on mortality in the acute respiratory distress syndrome, *N Engl J Med* 338 (6) (1998) 347-354.

[8] J. Villar, R.M. Kacmarek, L. Perez-Mendez and A. Aguirre-Jaime, A high positive end-expiratory pressure, low tidal volume ventilatory strategy

improves outcome in persistent acute respiratory distress syndrome: a randomized, controlled trial, *Crit Care Med* 34 (5) (2006) 1311-1318.

[9] K.C. Beck, J. Vettermann and K. Rehder, Gas exchange in dogs in the prone and supine positions, *J Appl Physiol* 72 (6) (1992) 2292-2297.

[10] M. Mure and S.G. Lindahl, Prone position improves gas exchange--but how?, *Acta Anaesthesiol Scand* 45 (2) (2001) 150-159.

[11] C. Allerod, S.E. Rees, B.S. Rasmussen, D.S. Karbing, S. Kjaergaard, P. Thorgaard and S. Andreassen, A decision support system for suggesting ventilator settings: retrospective evaluation in cardiac surgery patients ventilated in the ICU, *Comput Methods Programs Biomed* 92 (2) (2008) 205-212.

[12] D.S. Karbing, S. Kjaergaard, S. Andreassen, K. Espersen and S.E. Rees, Minimal model quantification of pulmonary gas exchange in intensive care patients, *Med Eng Phys* (2010)

[13] S.J. Verbrugge, B. Lachmann and J. Kesecioglu, Lung protective ventilatory strategies in acute lung injury and acute respiratory distress syndrome: from experimental findings to clinical application, *Clin Physiol Funct Imaging* 27 (2) (2007) 67-90.

[14] L. Gattinoni, F. Vagginelli, D. Chiumello, P. Taccone and E. Carlesso, Physiologic rationale for ventilator setting in acute lung injury/acute respiratory distress syndrome patients, *Crit Care Med* 31 (4 Suppl) (2003) S300-304.

[15] G. Hedenstierna, The hidden pulmonary dysfunction in acute lung injury, *Intensive Care Med* 32 (12) (2006) 1933-1934.

[16] L.N. Tremblay and A.S. Slutsky, Ventilator-induced lung injury: from the bench to the bedside, *Intensive Care Med* 32 (1) (2006) 24-33.

[17] S. Andreassen and S.E. Rees, Mathematical models of oxygen and carbon dioxide storage and transport: interstitial fluid and tissue stores and whole-body transport, *Crit Rev Biomed Eng* 33 (3) (2005) 265-298.

[18] B.J. Grant, Influence of Bohr-Haldane effect on steady-state gas exchange, *J Appl Physiol* 52 (5) (1982) 1330-1337.

[19] S.E. Rees and S. Andreassen, Mathematical models of oxygen and carbon dioxide storage and transport: the acid-base chemistry of blood, *Crit Rev Biomed Eng* 33 (3) (2005) 209-264.

[20] I. Tyuma, The Bohr effect and the Haldane effect in human hemoglobin, *Jpn J Physiol* 34 (2) (1984) 205-216.

[21] S. Andreassen, K.L. Steimle, M.L. Mogensen, J.B. de la Serna, S. Rees and D.S. Karbing, The effect of tissue elastic properties and surfactant on alveolar stability, *J Appl Physiol* 109 (5) (2010) 1369-1377.

[22] M.L. Mogensen, L.P. Thomsen, D.S. Karbing, K.L. Steimle, Y. Zhao, S.E. Rees and S. Andreassen, A Mathematical Physiological Model of the Dynamics of the Pulmonary Ventilation, *UKACC International Conference on CONTROL* 2010 September 7-10th, Coventry, UK (2010)

[23] K.L. Steimle, M.L. Mogensen, D.S. Karbing, J. Bernardino de la Serna and S. Andreassen, A model of ventilation of the healthy human lung, *Comput Methods Programs Biomed* 101 (2) (2010) 144-155

[24] M.L. Mogensen, D.S. Karbing and S. Andreassen, The effect of arteriolar resistance on perfusion distribution in a model of the pulmonary perfusion, *18th World Congress of the International Federation of Automatic Control (IFAC)* August 28 - September 2, Milano, Italy (2011)

[25] M.L. Mogensen, K.S. Steimle, D.S. Karbing and S. Andreassen, A model of perfusion of the healthy human lung, *Comput Methods Programs Biomed* 101 (2) (2010) 156-165

[26] S. Kjaergaard, S. Rees, J. Malczynski, J.A. Nielsen, P. Thorgaard, E. Toft and S. Andreassen, Non-invasive estimation of shunt and ventilation-perfusion mismatch, *Intensive Care Med* 29 (5) (2003) 727-734.

[27] G.M. Albaiceta, L. Blanch and U. Lucangelo, Static pressure-volume curves of the respiratory system: were they just a passing fad?, *Curr Opin Crit Care* 14 (1) (2008) 80-86.

[28] J.R. Axe and P.H. Abbrecht, Analysis of the pressure-volume relationship of excised lungs, *Ann Biomed Eng* 13 (2) (1985) 101-117.

[29] P.K. Behrakis, A. Baydur, M.J. Jaeger and J. Milic-Emili, Lung mechanics in sitting and horizontal body positions, *Chest* 83 (4) (1983) 643-646.

[30] P.K. Behrakis, B.D. Higgs, A. Baydur, W.A. Zin and J. Milic-Emili, Respiratory mechanics during halothane anesthesia and anesthesia-paralysis in humans, *J Appl Physiol* 55 (4) (1983) 1085-1092.

[31] L. Beydon, C. Svantesson, K. Brauer, F. Lemaire and B. Jonson, Respiratory mechanics in patients ventilated for critical lung disease, *Eur Respir J* 9 (2) (1996) 262-273.

[32] D.G. Markhorst, H.R. van Genderingen and A.J. van Vught, Static pressure-volume curve characteristics are moderate estimators of optimal airway pressures in a mathematical model of (primary/pulmonary) acute respiratory distress syndrome, *Intensive Care Med* 30 (11) (2004) 2086-2093.

[33] B.A. Simon, G.E. Christensen, D.A. Low and J.M. Reinhardt, Computed tomography studies of lung mechanics, *Proc Am Thorac Soc* 2 (6) (2005) 517-521, 506-517.

[34] O. Stenqvist, H. Odenstedt and S. Lundin, Dynamic respiratory mechanics in acute lung injury/acute respiratory distress syndrome: research or clinical tool?, *Curr Opin Crit Care* 14 (1) (2008) 87-93.

[35] J. Gil, H. Bachofen, P. Gehr and E.R. Weibel, Alveolar volume-surface area relation in air- and saline-filled lungs fixed by vascular perfusion, *J Appl Physiol* 47 (5) (1979) 990-1001.

[36] H. Rahn, A.B. Otis and et al., The pressure-volume diagram of the thorax and lung, *Am J Physiol* 146 (2) (1946) 161-178.

[37] J.C. Smith and D. Stamenovic, Surface forces in lungs. I. Alveolar surface tension-lung volume relationships, *J Appl Physiol* 60 (4) (1986) 1341-1350.

[38] R.S. Harris, Pressure-volume curves of the respiratory system, Respir Care 50 (1) (2005) 78-98; discussion 98-79.

[39] Q. Lu, S.R. Vieira, J. Richecoeur, L. Puybasset, P. Kalfon, P. Coriat and J.J. Rouby, A simple automated method for measuring pressure-volume curves during mechanical ventilation, *Am J Respir Crit Care Med* 159 (1) (1999) 275-282.

[40] A. Vieillard-Baron, S. Prin, J.M. Schmitt, R. Augarde, B. Page, A. Beauchet and F. Jardin, Pressure-volume curves in acute respiratory distress syndrome: clinical demonstration of the influence of expiratory flow limitation on the initial slope, *Am J Respir Crit Care Med* 165 (8) (2002) 1107-1112.

[41] C.L. Waltemath, N.A. Bergman and D.D. Preuss, Respiratory volume-pressure relationships during anaesthesia, *Can Anaesth Soc J* 20 (3) (1973) 281-289.

[42] Y. Zhao, S.E. Rees, S. Kjaergaard, B.W. Smith, A. Larsson and S. Andreassen, An automated method for measuring static pressure-volume curves of the respiratory system and its application in healthy lungs and after lung damage by oleic acid infusion, *Physiol Meas* 28 (3) (2007) 235-247.

[43] J.B. West, Importance of gravity in determining the distribution of pulmonary blood flow, *J Appl Physiol* 93 (5) (2002) 1888-1889; author reply 1889-1891.

[44] J.B. West, Regional differences in gas exchange in the lung of erect man, *J Appl Physiol* 17 (1962) 893-898.

[45] J.B. West and C.T. Dollery, Distribution of blood flow and ventilation-perfusion ratio in the lung, measured with radioactive carbon dioxide, *J Appl Physiol* 15 (1960) 405-410.

[46] G.M. Albaiceta, E. Piacentini, A. Villagra, J. Lopez-Aguilar, F. Taboada and L. Blanch, Application of continuous positive airway pressure to trace static pressure-volume curves of the respiratory system, *Crit Care Med* 31 (10) (2003) 2514-2519.

[47] J. Ingimarsson, L.J. Bjorklund, A. Larsson and O. Werner, The pressure at the lower inflexion point has no relation to airway collapse in surfactant-treated premature lambs, *Acta Anaesthesiol Scand* 45 (6) (2001) 690-695.

[48] P.M. Suter, B. Fairley and M.D. Isenberg, Optimum end-expiratory airway pressure in patients with acute pulmonary failure, *N Engl J Med* 292 (6) (1975) 284-289.

[49] J.T. Sharp, F.N. Johnson, N.B. Goldberg and P. Van Lith, Hysteresis and stress adaptation in the human respiratory system, *J Appl Physiol* 23 (4) (1967) 487-497.

[50] R.S. Harris, D.R. Hess and J.G. Venegas, An objective analysis of the pressure-volume curve in the acute respiratory distress syndrome, *Am J Respir Crit Care Med* 161 (2 Pt 1) (2000) 432-439.

[51] D.C. Grinnan and J.D. Truwit, Clinical review: respiratory mechanics in spontaneous and assisted ventilation, *Crit Care* 9 (5) (2005) 472-484.

[52] J.E. Parillo and R.P. Dellinger, Critical care medicine - Princlple of Diagnosis and Management in the Adult, (*Mosby*, 0-323-01280-9, 2002)

[53] B. Smith, S. Rees, J. Tvorup, C. Christensen and S. Andreassen, Modeling the influence of the pulmonary pressure-volume curve on gas exchange, *Conf Proc IEEE Eng Med Biol Soc* 3 (2005) 2357-2360.

[54] H.J. Schiller, J. Steinberg, J. Halter, U. McCann, M. DaSilva, L.A. Gatto, D. Carney and G. Nieman, Alveolar inflation during generation of a quasi-static pressure/volume curve in the acutely injured lung, *Crit Care Med* 31 (4) (2003) 1126-1133.

[55] R.D. Hubmayr, Perspective on lung injury and recruitment: a skeptical look at the opening and collapse story, *Am J Respir Crit Care Med* 165 (12) (2002) 1647-1653.

[56] J.H. Bates, Understanding lung tissue mechanics in terms of mathematical models, *Monaldi Arch Chest Dis* 48 (2) (1993) 134-139.

[57] J.H. Bates, A. Rossi and J. Milic-Emili, Analysis of the behavior of the respiratory system with constant inspiratory flow, *J Appl Physiol* 58 (6) (1985) 1840-1848.

[58] B. Jonson, L. Beydon, K. Brauer, C. Mansson, S. Valind and H. Grytzell, Mechanics of respiratory system in healthy anesthetized humans with emphasis on viscoelastic properties, *J Appl Physiol* 75 (1) (1993) 132-140.

[59] J. Milic-Emili, Pulmonary flow resistance, Lung 167 (3) (1989) 141-148.

[60] A.D. Bersten, A simple bedside approach to measurement of respiratory mechanics in critically ill patients, *Crit Care Resusc* 1 (1) (1999) 74-84.

[61] A.B. Lumb, Nunn's Applied Respiratory *Physiology*, (Butterworth-Heinemann, 0-7506-3107-4, 2003)

[62] S. Ganzert, K. Moller, D. Steinmann, S. Schumann and J. Guttmann, Pressure-dependent stress relaxation in acute respiratory distress syndrome and healthy lungs: an investigation based on a viscoelastic model, *Crit Care* 13 (6) (2009) R199.

[63] E. D'Angelo, E. Calderini, G. Torri, F.M. Robatto, D. Bono and J. Milic-Emili, Respiratory mechanics in anesthetized paralyzed humans: effects of flow, volume, and time, *J Appl Physiol* 67 (6) (1989) 2556-2564.

[64] E. D'Angelo, M. Tavola and J. Milic-Emili, Volume and time dependence of respiratory system mechanics in normal anaesthetized paralysed humans, *Eur Respir J* 16 (4) (2000) 665-672.

[65] E.R. Weibel, The pathway for oxygen, (*President and Fellows of Harvard College*, 0-674-65791-8, 1986)

[66] J. Lee Gde, Regulation of the pulmonary circulation, *Br Heart J* 33 (1971) Suppl:15-26.

[67] A. Despopulos and S. Silbernagl, Color atlas of phyisiology, (*Georg Thieme Verlag*, 3-13-545005-8, 2003)

[68] T.W. Secomb, Mechanics of blood flow in the microcirculation, *Symp Soc Exp Biol* 49 (1995) 305-321.

[69] R. Fahraeus and T. Lindqvist, The viscosity of blood in narrow capillary tubes, *Am J Physiol* 96 (1931) 562-568.

[70] A.R. Pries and T.W. Secomb, Rheology of the microcirculation, *Clin Hemorheol Microcirc* 29 (3-4) (2003) 143-148.

[71] A.R. Pries, T.W. Secomb and P. Gaehtgens, Biophysical aspects of blood flow in the microvasculature, *Cardiovasc Res* 32 (4) (1996) 654-667.

[72] U. Lucangelo, P. Pelosi, W.A. Zin and A. Aliverti, Respiratory System and Artificial Ventilation, (*Springer*, 978-88-470-0764-2, 2008)

[73] J.M. Hughes, J.B. Glazier, J.E. Maloney and J.B. West, Effect of lung volume on the distribution of pulmonary blood flow in man, *Respir Physiol* 4 (1) (1968) 58-72.

[74] L.H. Brudin, C.G. Rhodes, S.O. Valind, T. Jones and J.M. Hughes, Interrelationships between regional blood flow, blood volume, and ventilation in supine humans, *J Appl Physiol* 76 (3) (1994) 1205-1210.

[75] L.H. Brudin, C.G. Rhodes, S.O. Valind, T. Jones, B. Jonson and J.M. Hughes, Relationships between regional ventilation and vascular and extravascular volume in supine humans, *J Appl Physiol* 76 (3) (1994) 1195-1204.

[76] C.G. Rhodes, S.O. Valind, L.H. Brudin, P.E. Wollmer, T. Jones, P.D. Buckingham and J.M. Hughes, Quantification of regional V/Q ratios in humans by use of PET. II. Procedure and normal values, *J Appl Physiol* 66 (4) (1989) 1905-1913.

[77] S. Nyren, P. Radell, S.G. Lindahl, M. Mure, J. Petersson, S.A. Larsson, H. Jacobsson and A. Sanchez-Crespo, Lung ventilation and perfusion in prone and supine postures with reference to anesthetized and mechanically ventilated healthy volunteers, *Anesthesiology* 112 (3) (2010) 682-687.

[78] G. Hedenstierna, Pulmonary perfusion during anesthesia and mechanical ventilation, *Minerva Anestesiol* 71 (6) (2005) 319-324.

[79] P.D. Wagner, R.B. Laravuso, R.R. Uhl and J.B. West, Continuous distributions of ventilation-perfusion ratios in normal subjects breathing air and 100 per cent O2, *J Clin Invest* 54 (1) (1974) 54-68.

[80] R. Lisbona, G.W. Dean and T.S. Hakim, Observations with SPECT on the normal regional distribution of pulmonary blood flow in gravity independent planes, *J Nucl Med* 28 (11) (1987) 1758-1762.

[81] J. Petersson, M. Rohdin, A. Sanchez-Crespo, S. Nyren, H. Jacobsson, S.A. Larsson, S.G. Lindahl, D. Linnarsson, B. Neradilek, N.L. Polissar, R.W. Glenny and M. Mure, Posture primarily affects lung tissue distribution with minor effect on blood flow and ventilation, *Respir Physiol Neurobiol* 156 (3) (2007) 293-303.

[82] G. Musch, J.D. Layfield, R.S. Harris, M.F. Melo, T. Winkler, R.J. Callahan, A.J. Fischman and J.G. Venegas, Topographical distribution of pulmonary perfusion and ventilation, assessed by PET in supine and prone humans, *J Appl Physiol* 93 (5) (2002) 1841-1851.

[83] A.T. Jones, D.M. Hansell and T.W. Evans, Pulmonary perfusion in supine and prone positions: an electron-beam computed tomography study, *J Appl Physiol* 90 (4) (2001) 1342-1348.

[84] R.W. Glenny, W.J. Lamm, R.K. Albert and H.T. Robertson, Gravity is a minor determinant of pulmonary blood flow distribution, *J Appl Physiol* 71 (2) (1991) 620-629.

[85] M.N. Melsom, T. Flatebo, J. Kramer-Johansen, A. Aulie, O.V. Sjaastad, P.O. Iversen and G. Nicolaysen, Both gravity and non-gravity dependent factors determine regional blood flow within the goat lung, *Acta Physiol Scand* 153 (4) (1995) 343-353.

[86] R.W. Glenny, W.J. Lamm, S.L. Bernard, D. An, M. Chornuk, S.L. Pool, W.W. Wagner, Jr., M.P. Hlastala and H.T. Robertson, Selected contribution: redistribution of pulmonary perfusion during weightlessness and increased gravity, *J Appl Physiol* 89 (3) (2000) 1239-1248.

[87] K.S. Burrowes and M.H. Tawhai, Computational predictions of pulmonary blood flow gradients: gravity versus structure, *Respir Physiol Neurobiol* 154 (3) (2006) 515-523.

[88] G.R. Barer, P. Howard and J.W. Shaw, Stimulus-response curves for the pulmonary vascular bed to hypoxia and hypercapnia, *J Physiol* 211 (1) (1970) 139-155.

[89] R. Moudgil, E.D. Michelakis and S.L. Archer, Hypoxic pulmonary vasoconstriction, *J Appl Physiol* 98 (1) (2005) 390-403.

[90] N. Weissmann, N. Sommer, R.T. Schermuly, H.A. Ghofrani, W. Seeger and F. Grimminger, Oxygen sensors in hypoxic pulmonary vasoconstriction, *Cardiovasc Res* 71 (4) (2006) 620-629.

[91] R.C. Wetzel, C.J. Herold, E.A. Zerhouni and J.L. Robotham, Hypoxic bronchodilation, *J Appl Physiol* 73 (3) (1992) 1202-1206.

[92] D. Rimeika, S. Nyren, N.P. Wiklund, L.R. Koskela, A. Torring, L.E. Gustafsson, S.A. Larsson, H. Jacobsson, S.G. Lindahl and C.U. Wiklund, Regulation of regional lung perfusion by nitric oxide, *Am J Respir Crit Care Med* 170 (4) (2004) 450-455.

[93] I. Galvin, G.B. Drummond and M. Nirmalan, Distribution of blood flow and ventilation in the lung: gravity is not the only factor, *Br J Anaesth* 98 (4) (2007) 420-428.

[94] J.B. West, Distribution of pulmonary blood flow, *Am J Respir Crit Care Med* 160 (6) (1999) 1802-1803.

[95] R.W. Glenny, Determinants of regional ventilation and blood flow in the lung, *Intensive Care Med* 35 (11) (2009) 1833-1842.

[96] A. Ben-Tal, Simplified models for gas exchange in the human lungs, *J Theor Biol* 238 (2) (2006) 474-495.

[97] A.R. Kansal, Modeling approaches to type 2 diabetes, *Diabetes Technol Ther* 6 (1) (2004) 39-47.

[98] E.R. Carson and C. Cobelli, Modelling Methodology for Physiology and Medicine, (*Acedemic Press*, 0-12-160245-1, 2000)

[99] E.R. Carson, C. Cobelli and L. Finkelstein, The Mathematical Modeling of Metabolic and Endocrine System, (*John Wiley and Sons*, 0-471-08660-6, 1983)

[100] R.W. Glenny, Teaching ventilation/perfusion relationships in the lung, *Adv Physiol Educ* 32 (3) (2008) 192-195.

[101] C.E. Hahn and A.D. Farmery, Gas exchange modelling: no more gills, please, *Br J Anaesth* 91 (1) (2003) 2-15.

[102] M.P. Hlastala, A model of fluctuating alveolar gas exchange during the respiratory cycle, *Respir Physiol* 15 (2) (1972) 214-232.

[103] N.A. Bergman, Cyclic variations in blood oxygenation with the respiratory cycle, *Anesthesiology* 22 (1961) 900-908.

[104] B. Tawfik and H.K. Chang, A nonlinear model of respiratory mechanics in emphysematous lungs, *Ann Biomed Eng* 16 (2) (1988) 159-174.

[105] R.W. Jodat, J.D. Horgan and R.L. Lange, Simulation of respiratory mechanics, *Biophys J* 6 (6) (1966) 773-785.

[106] D. Stamenovic, K.R. Lutchen and G.M. Barnas, Alternative model of respiratory tissue viscoplasticity, *J Appl Physiol* 75 (3) (1993) 1062-1069.

[107] M. Thiriet, M. Bonis, A.S. Adedjouma, C. Hatzfeld and J.P. Yvon, Experimental and theoretical models of flow during forced expiration: pressure and pressure history dependence of flow rate, *Med Biol Eng Comput* 25 (5) (1987) 551-559.

[108] R.K. Lambert, T.A. Wilson, R.E. Hyatt and J.R. Rodarte, A computational model for expiratory flow, *J Appl Physiol* 52 (1) (1982) 44-56.

[109] K.H. Lin and G. Cumming, A model of time-varying gas exchange in the human lung during a respiratory cycle at rest, *Respir Physiol* 17 (1) (1973) 93-112.

[110] P. Poulsen, D.S. Karbing and S. Andreassen, Tidal breathing model describing end-tidal, alveolar, arterial and mixed venous CO2 and O2, *7th IFAC Symposium on Modelling and Control in Biomedical Systems (including Biological Systems)* (2009)

[111] A.A. Merrikh and J.L. Lage, Effect of blood flow on gas transport in a pulmonary capillary, *J Biomech Eng* 127 (3) (2005) 432-439.

[112] M.H. Tawhai, K.S. Burrowes and E.A. Hoffman, Computational models of structure-function relationships in the pulmonary circulation and their validation, *Exp Physiol* 91 (2) (2006) 285-293.

[113] C.H. Liu, S.C. Niranjan, J.W. Clark, Jr., K.Y. San, J.B. Zwischenberger and A. Bidani, Airway mechanics, gas exchange, and blood flow in a nonlinear model of the normal human lung, *J Appl Physiol* 84 (4) (1998) 1447-1469.

[114] J.G. Hardman and N.M. Bedforth, Estimating venous admixture using a physiological simulator, *Br J Anaesth* 82 (3) (1999) 346-349.

[115] J.G. Hardman, N.M. Bedforth, A.B. Ahmed, R.P. Mahajan and A.R. Aitkenhead, A physiology simulator: validation of its respiratory components and its ability to predict the patient's response to changes in mechanical ventilation, *Br J Anaesth* 81 (3) (1998) 327-332.

[116] J.G. Hardman, J.S. Wills and A.R. Aitkenhead, Factors determining the onset and course of hypoxemia during apnea: an investigation using physiological modelling, *Anesth Analg* 90 (3) (2000) 619-624.

[117] J.G. Hardman, J.S. Wills and A.R. Aitkenhead, Investigating hypoxemia during apnea: validation of a set of physiological models, *Anesth Analg* 90 (3) (2000) 614-618.

[118] J.B. West, Respiratory Physiology - The Essentials, (*Lippincott Williams & Wilkins*, 0-7817-5152-7, 2005)

[119] H. Bachofen, P. Gehr and E.R. Weibel, Alterations of mechanical properties and morphology in excised rabbit lungs rinsed with a detergent, *J Appl Physiol* 47 (5) (1979) 1002-1010.

[120] H. Itoh, M. Nishino and H. Hatabu, Architecture of the lung: morphology and function, *J Thorac Imaging* 19 (4) (2004) 221-227.

[121] K. Konno and J. Mead, Static volume-pressure characteristics of the rib cage and abdomen, *J Appl Physiol* 24 (4) (1968) 544-548.

[122] P. Lo, J. Sporring, H. Ashraf, J. Pedersen and M. de Bruijne, Vessel-guided airway segmentation based on voxel classification in 'Proc. of First International Workshop on Pulmonary Image Analysis, 978-1-4357-5952-7, 2008)

[123] A.B. Millar and D.M. Denison, Vertical gradients of lung density in healthy supine men, *Thorax* 44 (6) (1989) 485-490.

[124] F. Rohrer, Der Strömungswiderstand in den menschlichen Atemwegen und der Einfluss der unregelmässigen Verzweigung des Bronchialsystems auf den Atmungsverlauf in verschiedenen Lungenbezirken, *Pflüg. Arch. Ges. Physiol*. 162 (1915) 225-299.

[125] W.J. Beck, K.M.K. Muttzall and J.W.V. Heuven, Transport Phenomena, (*Wiley*, 0-471-99990, 2000)

[126] S.S. Sobin, Y.C. Fung, H.M. Tremer and T.H. Rosenquist, Elasticity of the pulmonary alveolar microvascular sheet in the cat, *Circ Res* 30 (4) (1972) 440-450.

[127] J.B. Glazier, J.M. Hughes, J.E. Maloney and J.B. West, Measurements of capillary dimensions and blood volume in rapidly frozen lungs, *J Appl Physiol* 26 (1) (1969) 65-76.

[128] J. Takala, Pulmonary capillary pressure, *Intensive Care Med* 29 (6) (2003) 890-893.

[129] S.R. Hopkins, T.J. Arai, A.C. Henderson, D.L. Levin, R.B. Buxton and G. Kim Prisk, Lung volume does not alter the distribution of pulmonary perfusion in dependent lung in supine humans, *J Physiol* 588 (Pt 23) (2010) 4759-4768.

[130] G.K. Prisk, K. Yamada, A.C. Henderson, T.J. Arai, D.L. Levin, R.B. Buxton and S.R. Hopkins, Pulmonary perfusion in the prone and supine postures in the normal human lung, *J Appl Physiol* 103 (3) (2007) 883-894.

[131] W.W. Wagner, Jr., L.P. Latham, W.L. Hanson, S.E. Hofmeister and R.L. Capen, Vertical gradient of pulmonary capillary transit times, *J Appl Physiol* 61 (4) (1986) 1270-1274.

[132] R.L. Capen, L.P. Latham and W.W. Wagner, Jr., Comparison of direct and indirect measurements of pulmonary capillary transit times, *J Appl Physiol* 62 (3) (1987) 1150-1154.

[133] R.G. Presson, Jr., W.A. Baumgartner, Jr., A.J. Peterson, R.W. Glenny and W.W. Wagner, Jr., Pulmonary capillaries are recruited during pulsatile flow, *J Appl Physiol* 92 (3) (2002) 1183-1190.

[134] R.G. Presson, Jr., J.A. Graham, C.C. Hanger, P.S. Godbey, S.A. Gebb, R.A. Sidner, R.W. Glenny and W.W. Wagner, Jr., Distribution of pulmonary capillary red blood cell transit times, *J Appl Physiol* 79 (2) (1995) 382-388.

[135] W.W. Wagner, Jr., L.P. Latham, M.N. Gillespie, J.P. Guenther and R.L. Capen, Direct measurement of pulmonary capillary transit times, *Science* 218 (4570) (1982) 379-381.

[136] P. Poulsen, D.S. Karbing, S.E. Rees and S. Andreassen, Tidal breathing model describing end-tidal, alveolar, arterial and mixed venous CO(2) and O(2), *Comput Methods Programs Biomed* 101 (2) (2010) 166-172

[137] H. Benallal, C. Denis, F. Prieur and T. Busso, Modeling of end-tidal and arterial PCO2 gradient: comparison with experimental data, *Med Sci Sports Exerc* 34 (4) (2002) 622-629.

[138] R. Casaburi, J. Daly, J.E. Hansen and R.M. Effros, Abrupt changes in mixed venous blood gas composition after the onset of exercise, *J Appl Physiol* 67 (3) (1989) 1106-1112.

[139] D. Linnarsson, Dynamics of pulmonary gas exchange and heart rate changes at start and end of exercise, *Acta Physiol Scand Suppl* 415 (1974) 1-68.

[140] A.H. Nickol, H. Dunroy, M.I. Polkey, A. Simonds, J. Cordingley, D.R. Corfield and M.J. Morrell, A quick and easy method of measuring the hypercapnic ventilatory response in patients with COPD, *Respir Med* 103 (2) (2009) 258-267.

[141] B. Jonson and C. Svantesson, Elastic pressure-volume curves: what information do they convey?, *Thorax* 54 (1) (1999) 82-87.

[142] K.G. Hickling, The pressure-volume curve is greatly modified by recruitment. A mathematical model of ARDS lungs, *Am J Respir Crit Care Med* 158 (1) (1998) 194-202.

[143] R. Glenny, Last word on Point:Counterpoint: Gravity is/is not the major factor determining the distribution of blood flow in the human lung, *J Appl Physiol* 104 (5) (2008) 1540.

[144] R. Glenny, Counterpoint: Gravity is not the major factor determining the distribution of blood flow in the healthy human lung, *J Appl Physiol* 104 (5) (2008) 1533-1535; discussion 1535-1536.

[145] M. Hughes and J.B. West, Last word on Point:Counterpoint: Gravity is/is not the major factor determining the distribution of blood flow in the human lung, *J Appl Physiol* 104 (5) (2008) 1539.

[146] P.D. Wagner, Point:Counterpoint: Gravity is/is not the major factor determining the distribution of blood flow in the human lung, *J Appl Physiol* 104 (5) (2008) 1537.

[147] S. Koyama, W.J. Lamm, J. Hildebrandt and R.K. Albert, Flow characteristics of open vessels in zone 1 rabbit lungs, *J Appl Physiol* 66 (4) (1989) 1817-1823.

[148] W.J. Lamm, K.R. Kirk, W.L. Hanson, W.W. Wagner, Jr. and R.K. Albert, Flow through zone 1 lungs utilizes alveolar corner vessels, *J Appl Physiol* 70 (4) (1991) 1518-1523.

[149] J.Y. Lu, J. Distefano, K. Philips, P. Chen and A.W. Neumann, Effect of the compression ratio on properties of lung surfactant (bovine lipid extract surfactant) films, *Respir Physiol* 115 (1) (1999) 55-71.

[150] J.M. Crane and S.B. Hall, Rapid compression transforms interfacial monolayers of pulmonary surfactant, *Biophys J* 80 (4) (2001) 1863-1872.

[151] H. Trauble, H. Eibl and H. Sawada, Respiration--a critical phenomenon? Lipid phase transitions in the lung alveolar surfactant, *Naturwissenschaften* 61 (8) (1974) 344-354.

[152] D.R. Otis, Jr., E.P. Ingenito, R.D. Kamm and M. Johnson, Dynamic surface tension of surfactant TA: experiments and theory, *J Appl Physiol* 77 (6) (1994) 2681-2688.

[153] C.G. Cochrane, Pulmonary surfactant in allergic inflammation: new insights into the molecular mechanisms of surfactant function, *Am J Physiol Lung Cell Mol Physiol* 288 (4) (2005) L608-609.

[154] H.J. Schiller, U.G. McCann, 2nd, D.E. Carney, L.A. Gatto, J.M. Steinberg and G.F. Nieman, Altered alveolar mechanics in the acutely injured lung, *Crit Care Med* 29 (5) (2001) 1049-1055.

[155] T.A. Wilson, Mechanics of the pressure-volume curve of the lung, *Ann Biomed Eng* 9 (5-6) (1981) 439-449.

[156] T.A. Wilson, Surface tension-surface area curves calculated from pressure-volume loops, *J Appl Physiol* 53 (6) (1982) 1512-1520.

[157] T.A. Wilson and H. Bachofen, A model for mechanical structure of the alveolar duct, *J Appl Physiol* 52 (4) (1982) 1064-1070.

[158] H. Kitaoka, G.F. Nieman, Y. Fujino, D. Carney, J. DiRocco and I. Kawase, A 4-dimensional model of the alveolar structure, *J Physiol Sci* 57 (3) (2007) 175-185.

[159] K.C. Beck and K. Rehder, Differences in regional vascular conductances in isolated dog lungs, *J Appl Physiol* 61 (2) (1986) 530-538.

[160] S.M. Walther, K.B. Domino, R.W. Glenny, N.L. Polissar and M.P. Hlastala, Pulmonary blood flow distribution has a hilar-to-peripheral gradient in awake, prone sheep, *J Appl Physiol* 82 (2) (1997) 678-685.

[161] L.A. Engel and M.M. Paiva, Gas mixing and distribution in the lung, (*Informa Healthcare*, 978-0824772840, 1985)

[162] O. Stenqvist and H. Odenstedt, Alveolar Pressure Volume Curves Reflect Regional Lung Mechanics, *Yearbook of Intensive Care and Emergency Medicine Part* 8 (2007) 407-414.

About the Author

Mads Lause Mogensen was born in Horsens on May 11, 1984, and grew up in Hovedgaard. After graduating from high school in 2003, he moved to Aalborg and started studying Biomedical Engineering at Aalborg University. There he was student assistant at the Center for Model-based Medical Decision Support. In June 2009 he obtained his M.Sc. degree after finishing a master thesis about mathematical models of the respiratory system, which was supervised by Steen Andreassen and Dan Stieper Karbing. The thesis resulted in two conference papers, which he presented at the 7th IFAC Symposium on Modeling and Control in Biomedical Systems in Aalborg. Mads continued afterwards his work on the respiratory system and presented some of it at biomedical conferences in Birmingham, England and Milan, Italy. Mads defended his Ph.D. thesis consisting of six papers the May 6, 2011 and was awarded his Ph.D. degree at Department of Health Science and Technology. Currently Mads is employed at Treat System A/S and participates in the development of a computerized decision support system for antibiotic treatment (TREAT).